In vivo adsorption of plasma proteins onto hydrogel coated silicone rubber: Evaluation using FT-IR/ATR

by

Linda Joanne Miller

A Thesis Submitted to the
Graduate Faculty in Partial Fulfillment of the
Requirements for the Degree of
MASTER OF SCIENCE

Major: Biomedical Engineering

Iowa State University
Ames, Iowa

1982

TABLE OF CONTENTS

LIST OF TABLES

LIST OF FIGURES

INTRODUCTION

When a foreign material is placed in contact with blood, a layer of proteins is rapidly deposited. This occurs in 3 to 5 seconds and is the initial step in the blood's response to contact with a foreign material. It has been determined that not only is this protein layer necessary for subsequent platelet deposition but that it can be used to predict the relative quantities of platelets that will adhere to the surface, depending on the nature and type of protein deposition.

Currently, considerable research is being conducted to characterize the protein layer. Experiments have been performed on many different materials to determine the rate and chronological sequence of deposition, as well as the molecular configuration and composition. By studying the protein layer, knowledge can be acquired about the body's response to foreign surfaces. It may be possible to formulate a material which, after an initial tolerance period, will be passivated and accepted by the body. Under some circumstances, it is desirable to prohibit the deposition of any proteins. This is the case for contact lenses, where any protein buildup causes discomfort to the wearer and inhibits vision.

This investigation assesses the blood's response to surfaces varying in hydrophilicity. Three formulations of

HEMA (hydroxyethyl methacrylate) and NVP (N-vinyl-pyrrolidone) were radiation grafted onto silicone rubber specimens. One advantage of hydrophilic surfaces is the low interfacial free energy that exists between the surface and an aqueous environment. Low interfacial free energy has been hypothesized to reduce the denaturation of proteins, and therefore to render the surface more compatible.

LITERATURE REVIEW

Hydrogels

More than twenty years ago, Wichterle and Lim (1960) began their work with hydrogels. Because of their hemo- and biocompatible properties, hydrogels are still under considerable investigation today. Hydrogels are a broad class of synthetic polymers which are able to swell in water and retain greater than twenty percent of the water in their structure without dissolving in the water (Hoffman et al., 1977). A list of their many uses in the field of medicine include coatings for sutures, catheters, intrauterine devices, vascular grafts, and electrophoresis cells, as well as homogeneous materials for electrophoresis cells, contact lenses, artificial corneas, breast implants, burn dressings, and hemodialysis membranes.

One of the disadvantages in utilizing hydrogels is their low mechanical strength. For many applications, they must be grafted onto a stronger support material. The hydrogels chosen for this investigation were HEMA and NVP. They were radiation grafted onto silicone rubber as the support material. In this manner, the surface characteristics of a material such as silicone rubber may be altered and possibly improved. By varying the solvent, percent monomer, and percent crosslinking agent, it is

possible to control the percent graft and associated water imbibition in the end product (Ratner and Hoffman, 1975). These parameters are of interest in efforts to design improved biomaterials.

Interfacial Phenomena

Surface Tension

At the surface of matter, especially liquids, there exist asymmetric forces which pull the surface molecules inward. The number of surface molecules continues to decrease until a minimum surface area is reached. The tension created at the surface due to the depletion of molecules is called surface tension and is expressed as dynes/cm (Andrade, 1973).

Surface Free Energy

Surface energy is a measure of the inward forces that result in unsatisfied bonds at the surface. It is expressed in ergs/cm^2 and is therefore equivalent to surface tension.

Interfacial Free Energy

When two surfaces, each with its particular surface free energy, contact each other, the unsatisfied bonds are satisfied, and the surface energy is reduced. The interfacial free energy can be described by $\gamma AB=\gamma A-\gamma A(B)+\gamma B-\gamma B(A)$, where γAB=the interfacial energy,

γA=the surface free energy of A, γB=the surface free energy of B, $\gamma A(B)$ = the effect of B on A, and $\gamma B(A)$ =the effect of A on B (Andrade, 1973). Holly (1979) claims that solids with low surface energy in air usually have high interfacial tension in water. Conversely, materials that have low interfacial tension in water have high surface free energy.

Contact Angle

Depending on the interfacial energy, a liquid drop placed on a solid surface will either bead or spread over the surface. A line tangent to the drop forms the contact angle. If the contact angle is greater than 90°, the surface is hydrophobic. However, if the contact angle is less than 90°, the liquid will spread over the surface until at contact angle equal zero, the surface becomes completely wet. This surface is hydrophilic. The contact angle provides an inverse measure of wettability (Andrade, 1973).

As can be seen from the contact angle data in Figure 1, for HEMA and NVP, polymerized in 12% methanol and 68% water by gamma irradiation, 10% HEMA/10% NVP is the most hydrophilic, 15% HEMA/5% NVP is next, and 5% HEMA/15% NVP is the least hydrophilic of the series. The water contact angle for silicone rubber is 103°.

Some investigators prefer using advancing and receding contact angles on hydrogels instead of the sessile drop method described above. Large hysteresis has been observed

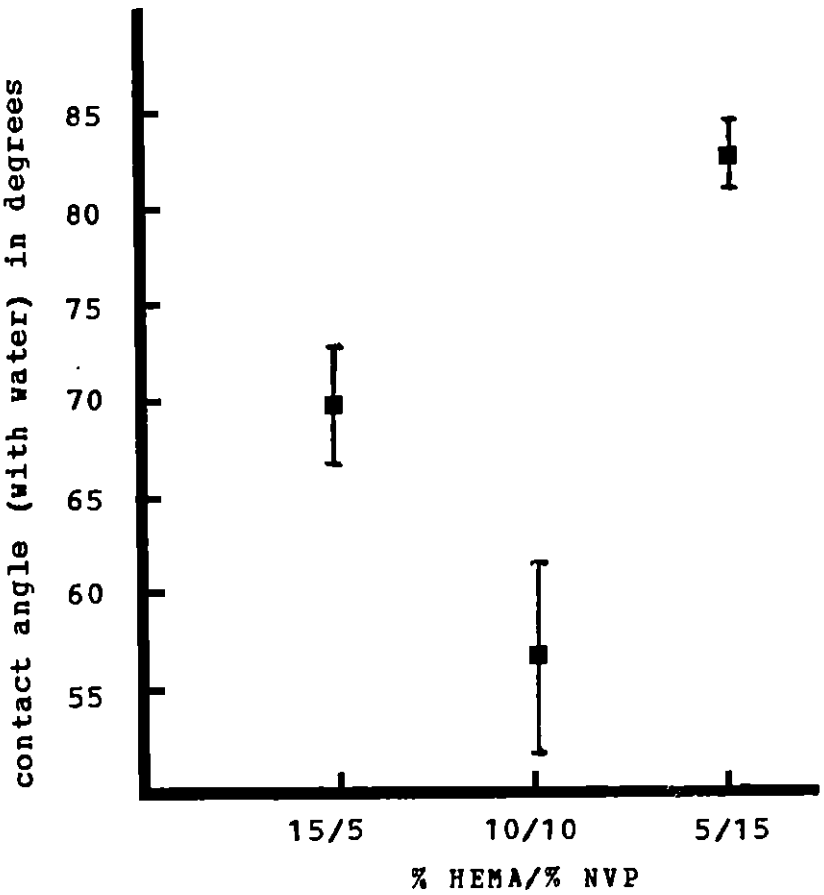

FIGURE 1. Contact angle data (Vale, 1980, pg. 94)

in this method, and this is believed to be due to reorientation of the polymer backbone (Holly and Refojo, 1975, 1976). Hydrogels can have low surface free energy at an interface with air, water vapor, or nonpolar liquids by orienting the hydrophobic (i.e., methyl) groups outward. Likewise, they can have low interfacial tension in water by orienting the hydrophilic (i.e., hydroxyl) groups outward

(Holly, 1979).

Critical Surface Tension

If the contact angle of a series of liquids which vary in surface tension (shown as $\cos\theta$), is plotted against surface tension of the liquid, a linear relationship will result. Extrapolation of the line to $\cos\theta=1$ yields the critical surface tension. Critical surface tension values of 20 to 30 dynes/cm are considered to represent values for materials which would be biocompatible (Baier, 1977). Lyman et al. (1969) have observed decreasing platelet adsorption with decreasing critical surface tension of different materials.

Structured Water

Not only is the quantity of water an important consideration for the initial adsorption of proteins on a hydrophilic surface, but also the structure and organization of water (Andrade et al., 1973; Garcia et al., 1980). Jhon and Andrade (1973) claim that there are at least three kinds of water in hydrogels: (1) hydrated, (2) interfacial, and (3) bulk. Other investigators (Nakashima et al., 1977) have discovered only two kinds of water: (1) free, and (2) bound to the polymer directly by hydrogen bonds and indirectly to other water molecules. Nakashima et al. (1977) claim that at the interface between blood and a solid surface, water

near the hydrophobic sites on the solid surface may form "iceberg" structures while water near the hydrophilic sites may be bound to the surface. Iceberg formation refers to the hydrophobic character of a hydrocarbon molecule which causes the water molecules to organize around it and to case it in an icelike casing. They further suggest that water bound to the hydrophilic sites may inhibit iceberg formation (i.e., the hydrophobic domain is dispersed in the hydrophilic matrix and the high amount of water bound in the polymer) and in this manner inhibit blood coagulation.

Time Sequence of Deposition

Although there is considerable debate concerning the exact sequence of events that occurs when blood contacts a foreign surface, most investigators agree on the basic sequence: polymer surface-blood contact, competitive adsorption of plasma proteins, formation of protein coated surface, platelet approach, platelet reaction with glycoproteins, platelet adhesion, thrombus and coagulation (Kim et al., 1974).

Baier (1977) believes that platelet morphology is the first signal that a thromboresistant surface has been contacted. The platelets will be round with few pseudopods and no degranulation. Within a few minutes after platelet adherence, chemotactic stimulation of white cells toward the

surface is observed. The white cells cover the platelets and, through some poorly understood mechanism, phagocytize the platelets. He also postulates that the white cells may release enzymes which loosen and cause sloughing of the protein film. In contrast, Barber et al. (1979) have observed leucocyte adherence, specifically neutrophils and monocytes, preceding thrombus and conclude that initial leucocyte adherence may be a critical factor for thrombus to occur on certain surfaces.

In more recent studies, the Battelle Research Laboratories group using Fourier Transform Infrared Spectroscopy (FT-IR) with an Attenuated Total Reflectance (ATR) accessory and flowing whole blood has determined the sequence of protein deposition onto a germanium crystal (Gendreau et al., 1981). Initially, albumin is adsorbed as the primary component. Immediately following albumin adsorption is the adsorption of a highly labile carbohydrate species, which adsorbs and desorbs rapidly. Still within the first few minutes, fibrinogen and possibly gamma globulins replace albumin as the predominant adsorbing species. Similar results were observed on Biomer®, silicone rubber and polyvinylchloride with the following exceptions: Biomer®adsorbed the least protein, and silicone rubber adsorbed and desorbed the most. Silicone rubber adsorbed four times as much glycoprotein as Biomer®and

polyvinylchloride (Gendreau et al., ca. 1982a).

Compositional Changes

Plots as a function of time of protein bands which are common to all proteins (1550 and 1400 cm^{-1}) indicate that adsorption occurs quickly with over half the total protein adsorbed in 15 seconds and over 90 percent in 30 seconds (Jakobsen et al., ca. 1982b). After adsorption levels off, the primary proteins begin to be replaced. During this exchange, the total protein remains constant (Gendreau et al., 1981).

Molecular Configuration

Brash and Uniyal (1979) claim that there is a wide variation in characteristics of protein adsorption to different surfaces. Using radioiodine labeling, they observed the formation of closely packed monolayers of protein, but could find no more than single layers formed on solid surfaces. In direct conflict are the observations of many other investigators (Dillman and Miller, 1973; Bagnall, 1977; Watkins and Robertson, 1977) who have observed at least two layers. Early work by Lyman et al. (1968) and Brash and Lyman (1969) using infrared (IR) internal reflection, calculated an end on configuration of the protein molecules, indicating that the proteins remain globular, i.e., they are not denatured on nonwettable

solids. This conflicts with later results by Bagnall (1977), who states that because globular proteins have hydrophobic cores and hydrophilic surfaces, adsorption on hydrophobic surfaces will cause molecular distortion as the molecule unfolds trying to present as nonpolar a surface as possible to minimize interfacial tension. Sometimes this may not be possible because of internal constraints on the molecule. In addition, the possibility of an initially adsorbed denatured layer, followed by a layer of proteins in their native state has been proposed (Brash and Lyman, 1969; Bagnall, 1977). The denatured layer, in this case, would be in contact with the polymer while the native protein layer would be exposed to blood.

Conformational Changes

The conformation of the adsorbed protein layer is believed to be important in the determination of biocompatibility (Jakobsen and Gendreau, 1978). The term, conformation, refers to the secondary structure of the protein, i.e., alpha helix, beta sheet, or random coil. Albumin tends to be a mixture of alpha helix (55%), beta pleated sheets (15%), and random coil (30%). Fibrinogen is composed of alpha helix (30-50%), random coil (60%), and beta sheet (5-10%) (Gendreau et al., ca. 1982b). Environmental factors such as pH and concentration can produce conformational changes in protein structure. These

changes can be observed in the IR spectrum.

Reversible vs Irreversible

In general, hydrophilic surfaces adsorb less protein than hydrophobic surfaces (Holly, 1979; Brash and Uniyal, 1979; Lyman et al., 1969; Andrade, 1973), and the protein adsorbed to the hydrophilic surface is reversibly bound (Bagnall, 1977; Lyman et al., 1969; Holly, 1979). Weathersby et al. (1977) report that the 'loose fraction' constituted approximately 25 percent of the adsorbed fibrinogen on HEMA grafts, but only 5 percent on surfaces containing at least 5 percent EMA (ethyl methacrylate). In addition, the 'strongly bound' fibrinogen desorbs twice as fast from HEMA as from EMA. Therefore, protein adsorption on a hydrophilic surface is reversible while adsorption on a hydrophobic surface is irreversible. Relating this to the previously discussed concept of multilayer adsorption, the initial layer is irreversibly bound but the second layer is loose and can be desorbed (Gendreau and Jakobsen, 1979; Bagnall, 1977; Dillman and Miller, 1973; Watkins and Robertson, 1977). Watkins and Robertson (1977) determined that the amount of loosely held protein is proportional to the bulk protein concentration, but warn that this may not be true at physiological concentrations. Therefore, the surface eventually exposed to blood is not the artificial

material or even the tightly adsorbed layer (which may be denatured), but rather the loose layer of native proteins.

In their FT-IR/ATR experiments, the Battelle Research Laboratories group (Jakobsen et al., ca. 1982a) has observed that increasing the flowrate of pure albumin solutions, while maintaining the same concentration, or decreasing the concentration at the same flowrate, decreases the amount adsorbed. Therefore, the amount adsorbed is directly proportional to concentration and inversely proportional to flowrate. In similar desorption experiments, they noted the smaller the quantity adsorbed, the smaller the amount desorbing. Therefore, the total amount desorbed is inversely proportional to the flowrate during adsorption and directly proportional to the concentration during adsorption, i.e., at faster flowrates, less protein adheres but it adheres more tightly.

Type of Protein

An adsorbed protein coat determines and is a necessary precursor for platelet adhesion (Kim et al., 1977). Some of the earliest work in protein adsorption consisted of precoating different surfaces with various proteins before exposing them to whole blood or blood components (Packham et al., 1969). In later experiments the uncoated surface was exposed (Ihlenfeld and Cooper, 1979). Results consistently

show that surfaces which adsorb or are precoated with albumin attract fewer platelets and the surface becomes passivated (Packham et al., 1969; Lyman et al., 1974; Vroman et al., 1977; Barber et al., 1979). If fibrinogen is the main protein adsorbed, the surface will attract more platelets and can become thrombogenic or thromboembolic (Mason et al., 1971; Packham et al., 1969; Lee and Kim, 1974; Roohk et al., 1976). Gamma glubulins have also been shown to attract an increased number of platelets (Roohk et al., 1977).

Studies conducted using mixed protein solutions indicate that proteins are not adsorbed in proportion to their concentrations in the bulk solution, i.e., surfaces selectively attract specific proteins (Horbett and Hoffman, 1975; Kim et al., 1974; Lee et al., 1974).

Protein Spectral Characteristics

Table 1 lists the locations and relative intensities of IR bands for albumin (Koenig and Tabb, 1980) and fibrinogen (Gendreau and Jakobsen, 1979). The IR spectrum for fibrin is very similar to that of fibrinogen (Jakobsen et al., 1981).

TABLE 1. Infrared Bands (cm^{-1}) for Albumin and Fibrinogen

albumin film	fibrinogen film
1656 vs	1650 vs
1540 s	1550 s
1452 m	1450 m
1390 m	1400 m
	1320 w
1305 m	
1248 w	1240 m
1172 w	1160 vw
	1080 w

vs=very strong, s=strong, m=moderate, w=weak, vw=very weak

Mechanisms for Platelet Attachment

Lee and Kim (1974) have proposed a mechanism for platelet attachment which involves the formation of enzyme-substrate complex bridges between platelet glycosyl transferases and incomplete heterosaccharides in glycoproteins. Assays were conducted utilizing three plasma proteins: albumin, fibrinogen, and gamma globulins, and two platelet glycosyl transferases: sialyl transferase and galactosyl transferase. When the proteins were treated (sialic acid or galactose removed), fibrinogen and gamma globulin coated surfaces showed greater platelet adherence than either surface untreated. Treated and untreated albumin coatings reacted the same since albumin is not a glycoprotein. These findings are consistent with those of Jakobsen and Gendreau (1978) who observed that the ratio of

carbohydrate to protein is significantly higher on thrombogenic surfaces than on thromboresistant. Kim et al. (1977) have also postulated that adsorbed fatty acid salts are released from the interface following contact with plasma to form localized concentrations of fatty acids which cause platelet aggregation.

Techniques used to Study the Protein Layer

In the past, researchers have employed many methods to study protein adsorption and the resulting platelet adherence. As previously mentioned, in some studies surfaces were precoated with individual proteins (Packham et al., 1969; Lee and Kim, 1974). Others have studied adsorption from single protein solutions (Horbett and Hoffman, 1975; Kim and Lee, 1975). Adsorption from mixtures indicates decreased surface concentrations (Brash and Uniyal, 1976) of proteins compared with adsorption from single protein solutions. Varying flowrate studies show greater adsorption from static systems than from flowing systems (Gendreau and Jakobsen, 1979). Brash and Uniyal (1976) reported a decrease in surface concentrations upon the addition of washed red cells. Radiolabels have been used extensively in in vitro and in vivo experiments (Ihlenfeld and Cooper, 1979; Weathersby et al., 1977; Barber et al., 1978, 1979; Brash and Uniyal, 1979; Roohk et al.,

1976). Lyman et al. (1974) and Weathersby et al. (1976) used elution methods.

IR and internal reflection techniques were used in early investigations (Lyman et al., 1968; Brash and Lyman, 1969; Baier and Dutton, 1969). Watkins and Robertson (1977) used ATR to study the adsorption of fluorescein labelled gamma globulin onto silicone rubber. Kim and Lee (1975) employed internal reflection IR spectroscopy in their studies of adsorption of single protein solutions onto hydrophobic polymers. The Battelle Research Laboratories group has utilized FT-IR/ATR to investigate adsorption from single solutions (Gendreau et al., ca. 1982b; Jakobsen et al., ca. 1982a), mixed solutions (Gendreau et al., ca. 1982b; Gendreau and Jakobsen, 1979; Jakobsen et al., ca. 1982a), and static and flowing solutions (Gendreau and Jacobsen, 1979). They have extensively studied adsorption from flowing whole blood onto a germanium crystal and, to a limited extent, onto various polymer thin films including silicone rubber, Biomer, polyethylene, and polyvinylchloride (Gendreau and Jacobsen, 1979; Gendreau et al., 1981; Jakobsen et al., ca. 1982b).

FT-IR/ATR

A brief description of the techniques used in this investigation, FT-IR and ATR, is necessary. Attenuated

total reflection (ATR) is based on the principle of total internal reflection. When a beam of radiation is passed into a prism, for example germanium, the energy is totally reflected from the back face, then the front face, and so on until the beam emerges from the opposite end of the prism. The sample to be examined is placed in intimate contact with the crystal. As the beam passes through the crystal, energy at the points of reflection is selectively absorbed by the sample so the resulting spectrum is characteristic of the sample. The beam penetrates approximately 6000A (for a 60° germanium prism) into the sample, but penetration varies depending on the specific prism used and the angle of incidence. The intensity of the IR radiation of a given frequency depends on the refractive index, angle of incidence, and the absorption index (Conley, 1972, pg. 57). The technique is useful for, but not limited to, the IR examination of solid materials. One advantage it has over conventional IR is the ability to analyze opaque samples since the resulting spectrum is independent of sample thickness; therefore, the need for precise and extremely short path length cells is eliminated. When ATR is coupled with FT-IR, an extremely sensitive system is produced. The spectrum generated by the interferogrammed light is Fourier Transformed into an IR spectrum. FT-IR employs a minicomputer for data processing. The improved signal to

noise ratio of the FT over conventional IR greatly improves the usefulness of the ATR technique. The computer allows for spectral manipulations such as addition, subtraction, and scaling. By subtracting spectra of known samples from that of an unknown sample, it is possible to identify the components of the original spectrum. In this way larger peaks in a mixed sample can be subtracted, making smaller shoulder peaks more prominent. In the case of protein deposition onto a crystal or coated crystal surface, spectral stripping can remove all spectral components except that characteristic of the deposit.

MATERIALS AND METHODS

Materials

The monomer 2-hydroxyethyl methacrylate (LOT B889F9) was obtained from Alcolac, Inc., 3440 Fairfield Rd., Baltimore, Maryland and was used as received. N-vinyl-2-pyrrolidone (LOT 236-12) was obtained from Monomer-Polymer and Dajak Labs, Inc., 36 Terry Drive, Trevose, Pennsylvania, and was used as received. Dow Corning silicone rubber tubing (LOT H118338, 0.132 in ID x 0.183 in OD, and LOTS H040101, H070406, 0.078 in ID x 0.125 in OD) and silicone rubber sheeting (LOT H059172) were purchased from GenTec Health Care, Inc., 1285 Thomas Road, Des Moines, Iowa.

Vacuum tubes (Vacutainer #3865), containing 12 mg of siliceous earth, and vacuum tubes (Vacutainer #3206Q), containing 6 mg of sodium EDTA, an anticoagulant, were obtained from Becton-Dickinson, Division of Becton, Dickinson and Company, Rutherford, New Jersey, and were used for ACT (activated clotting time) and platelet counts, respectively. Sodium pentobarbital and Sleepaway were obtained from Fort Dodge Laboratories, Fort Dodge, Iowa. Blood for platelet counts was diluted using 20 μl capillary pipettes (LOT 9B722) and 1.98ml Unopette reservoirs (LOT 9C5971Q) from Becton-Dickinson, Rutherford, New Jersey.

Platelets were counted on a Spencer "Bright Line" hemacytometer (cat. 1492) made by AO Instrument Company, Buffalo, New York. Suture material was acquired from Ethicon, Inc., Somerville, New Jersey. Silastic Medical Adhesive Silicone Type A (LOT H010503) was acquired from Dow Corning Corporation Medical Products, Midland, Michigan.

Microscopic examination of the blood exposed surfaces was performed on a JEOL-U3 Scanning Electron Microscope (SEM), Japanese Electron Optics, Tokyo, Japan. Samples were dried in a Polaron critical point drier (E3000) and sputter coated with a Polaron SEM coating unit (E5100), Polaron Instruments, Inc., Warrington, Pennsylvania. The carbon paint was obtained from Acheson Colloids Co., Port Huron, Michigan.

FT-IR evaluations were performed on an IBM IR-98 FT-IR, IBM Instruments, Inc., Danbury, Connecticut. The 60° Germanium ATR prism and ATR solid sample holder were also obtained from IBM Instruments. Micro cleaner and hexanes for cleaning the analyzing crystals were generously supplied by Instrument Services, Iowa State University, Ames, Iowa.

Methods

Method 1- Sample Preparation (Tubing)

Silicone rubber tubing was washed in a mild solution of Ivory Flakes for 10 minutes in an ultrasonic cleaner,

ultrasonically rinsed in deionized water for 10 minutes, rinsed in distilled water and air dried. Four foot sections were filled with the appropriate nitrogen degassed monomer-solvent solution (5% HEMA/15% NVP/15% methanol[1] ; 10% HEMA/10% NVP/15% methanol; 15% HEMA/5% NVP/15% methanol), tied securely at both ends, and irradiated in a ^{60}Co source. The dose was 2500 Grays (0.25 Mrad). Following irradiation, the tubing samples were filled with a 1:1 solution of ethanol and water to remove any unpolymerized monomer. This solvent was changed several times prior to storage of the tubing samples in a fresh aliquot of solvent. Twenty-four hours prior to surgery the tubing samples were filled with saline.

Implantation

Dogs weighing 25-30 kg were obtained from Laboratory Animal Resources, Iowa State University, Ames, Iowa. The animals were fasted overnight and anesthetized with an intravenous injection of sodium pentobarbital (29 mg/1 kg body weight). Additional anesthesia was administered as needed. Presurgical blood specimens were drawn for platelet counts. The anesthetized animals were placed in a supine position with the legs extended. Nonsterile technique was used.

---

[1] i.e., 5% HEMA/15% NVP/15% methanol/65% water

A 10-12 centimeter incision was made directly external to the femoral artery and vein. Using blunt dissection, the tissues were separated to expose the blood vessels. An ex vivo, unilateral shunt was constructed by cannulating both the femoral artery and femoral vein. A two foot section of one type of experimental tubing was inserted and was maintained with two ligatures around each vessel. Patency of the shunt was monitored every 5 minutes with a Parks 806 Doppler Ultrasound flowmeter. The tubing sample was left in place for 45 minutes, or until no flow was detected. After removal, the section was flushed gently with saline to remove excess blood without stripping adhering deposits from the wall. A one inch section was fixed in 2% glutaraldehyde for subsequent SEM analysis, while the remainder of the tubing was air dried prior to FT-IR analysis. This procedure was repeated in the animal for the remaining three types of tubing. Samples for FT-IR analysis were examined as soon as possible after the surgery.

Sample Analysis

Microscopic evaluations were made using scanning electron microscopy. Following fixation in glutaraldehyde, the sections were dehydrated in a series of acetone rinses (30, 60, 75, 90, 100, and 100% v/v), critical point dried, mounted on aluminum stubs using carbon paint, coated with 300A gold, and examined.

Half-inch sections of tubing were slit longitudinally through both sides with a scalpel blade. One section was firmly placed in the center on each side of a 45° KRS-5 ATR prism in the solid sample holder. IR spectra were collected with an IBM IR-98 FT-IR and a variable angle ATR accessory.

Method 2- Sample Preparation (Sheets)

Surfaces varying in hydrophilicity were prepared by radiation grafting various formulations of HEMA and NVP monomers onto silicone rubber sheeting. Silicone rubber sheeting (0.02 mm thick), and twelve 12cc syringes were ultrasonically washed in a mild solution of Ivory Flakes for 10 minutes, ultrasonically rinsed for 10 minutes in deionized water, rinsed in distilled water, and air dried. Scintillation vials were filled with the appropriate nitrogen degassed monomer-solvent solution (5% HEMA/15% NVP/15% methanol; 10% HEMA/10% NVP/15% methanol; 15% HEMA/5% NVP/15% methanol). 10x50 mm strips of silicone rubber sheeting were suspended in the solutions and exposed to 2500 Grays (0.25 Mrad) irradiation in a ^{60}Co source. The silicone rubber sheets were stripped from the bulk polymer and immersed in a solution of 1:1 ethanol/water for several days. Twice daily the sheets were vigorously scrubbed with gauze sponges soaked in 1:1 ethanol/water until no more "lumps" of bulk polymer were visible. The samples were stored in distilled water.

Flowcell Preparation

Twelve 12cc polypropylene syringes were cut, six at the 12 cc mark and six at the 8 cc mark. Each syringe was attached to a 1 foot length of silicone rubber tubing (0.078 in ID x 0.125 in OD) by means of a cuff formed from a half inch piece of silicone rubber tubing (0.132 in ID x 0.183 in OD). The cuff was strengthened by the addition of a small bead of Silastic Medical Adhesive Silicone Type A and allowed to dry overnight. To minimize surface material interactions inside the flowcell, each syringe assembly was coated with a thin layer of silicone rubber. The syringe assemblies were held vertically and immersed approximately one half inch below the surface of a solution composed of a 6 inch bead of Silastic Medical Adhesive Silicone Type A well mixed with 60 cc of hexanes. A 50cc syringe at the upper end of the tubing was used to draw the solution into the syringe. After removal from the silicone rubber/hexanes solution, each syringe was blotted several times at the open end, and hung vertically to dry for several days. A uniformly thin coating of silicone rubber with no visible drips was produced on the inside of each syringe. Twenty-four hours prior to surgery, the hydrogel grafted silicone rubber samples were fastened in a circle at the open end to the inside of the longer syringe by coating one side of each sample with Silastic Medical Adhesive Silicone Type A and

gently pressing it into place with a wooden applicator stick soaked in saline. The samples were arranged counterclockwise in the following order, silicone rubber, 5% HEMA/15% NVP, 10% HEMA/10% NVP, 15% HEMA/5% NVP. In this manner, four surfaces varying in hydrophilicity could be simultaneously exposed to flowing blood. On the morning of surgery, the longer syringe with the attached samples was joined to the shorter syringe using a half inch piece of silicone rubber as a cuff. This created a flowcell with the samples equidistant from the two ends. The entire system was filled with saline and clamped at both ends.

Implantation

Dogs weighing 25-33 kg were obtained from Laboratory Animal Resources, Iowa State University. The surgical procedure used in method 1 was followed except both hind legs were used. Presurgical blood specimens were drawn for platelet counts and ACT (activated clotting time). The left femoral vessels were exposed first and covered with saline soaked gauze to prevent tissue drying while the procedure was repeated on the right leg. The flowcell assembly was inserted vertically so the blood flowed from the artery, up through the flowcell, and back to the vein. The flowcell was inserted in the right leg first. After 15 minutes, the right femoral artery and vein were clamped with bulldog clamps cranial to the cannulation site, the tubings leading

to and from the flowcell cut, and the flowcell opened to facilitate rinsing the lumen in several changes of saline. Fifteen minutes was arbitrarily chosen for the time of exposure to blood. The syringe with samples was stored in saline until the end of the experiment. The procedure was repeated for the left leg. At the end of the experiment, the samples were pried loose by carefully inserting a screwdriver under each sample. As quickly as possible, the samples were cut in half. One section was suspended with suture material and fixed in glutaraldehyde while the other was allowed to air dry. Again the samples for FT-IR were analyzed as soon as possible following surgery.

Sample Analysis

Microscopic evaluations were made as in Method 1.

IR spectra were collected with an IBM IR-98 FT-IR and a variable angle ATR accessory. The parameters used to collect, store, and plot the spectra are listed in Appendix A. A polished 60° germanium crystal was used for all samples. Samples which had been exposed to blood were placed firmly in contact with one side of the crystal in a solid sample holder.

Prior to sample analysis, several preliminary experiments were run. The first set of experiments consisted of removing the crystal and sample holder and replacing it either with or without using the chopper for

alignment. This was to determine whether accurate alignment could be produced without using the chopper for alignment. The next set of experiments involved placing 10x2.5 mm sheets of silicone rubber on the crystal and tightening the sample holder to varying degrees to determine the effect on the spectrum of pressure on the sample.

For analysis of those samples which had been exposed to blood, 5x10 mm sections were used. Prior to beginning each new sample set, the germanium crystal was cleaned with a cotton ball soaked in Micro cleaner diluted with distilled water, and thoroughly rinsed in distilled water. In between samples, the crystal was cleaned with hexanes and a Kimwipe. A spectrum of the clean crystal (e.g., LIND54) was collected before each new set of samples was run. Each blood exposed sample was applied firmly to the crystal and a spectrum was collected.

Spectral Subtractions

Since, during the collection of a spectrum, the beam sees the protein layer and the underlying polymer, it is necessary to subtract the polymer spectrum. This was done by collecting spectra of silicone rubber, 5% HEMA/15% NVP, 10% HEMA/10% NVP, and 15% HEMA/5% NVP and subtracting them from the spectra of the appropriate protein coated samples using one of the subtract programs provided by IBM (see Appendix B).

After the completion of the experiment, it was discovered that the high frequency component of the spectra between 1800 and 1400 wavenumbers was due to water in the sample. To remove this interference, a spectrum of water vapor was collected, stored, and subtracted from the appropriate spectra. The water vapor spectrum was collected by placing several drops of water on the germanium crystal. Since the IBM system used in this investigation is under vacuum, the water placed on the crystal dissipates as soon as the system pumps down. The spectrum collected represents water vapor in the two meter beam path.

Two methods were utilized for the necessary subtractions. In the first method, water vapor (LIND93) was subtracted from the "wet" protein coated polymer (LIND56) using the SSM (subtract spectrum manual) command. The SSM real time subtract program determines the subtraction constant (CON) by subtracting the file assigned to AFB (e.g., LIND93) from the file assigned to AFA (e.g., LIND56) while using the file assigned to AFC (e.g., LIND54) as a common reference. The value of CON is automatically stored in the computer memory by the software. With AFN set equal to SS (see Appendix B), the "dry" protein coated polymer (DLIND56) was stored as a new file. The SS equation performs the actual subtraction by using the equation,

-log(SCAxAFA)/(SCCxAFC)-CON(-log((SCBxAFB)/(SCCxAFC))),

where the parameters AFA, AFB, and AFC have been appropriately set, and CON has been determined by the real time subtract program. Next, water vapor was subtracted from the "wet" polymer (LIND55). With AFN equal to SS, the "dry" polymer was stored as (DLIND55). Finally, by subtracting the "dry" polymer (DLIND55) from the "dry" protein coated polymer (DLIND56) using the SAM (subtract absorbance manual) command, only the "dry" protein remains. AFN is set equal to AS to plot the resulting spectrum. The AS equation subtracts two absorbance files. Figure 2 illustrates the above text in equation form.

SSM# $\frac{\text{LIND56}}{\text{LIND54}} - \frac{\text{LIND93}}{\text{LIND54}}$ AFN=SS stored as DLIND56

SSM# $\frac{\text{LIND55}}{\text{LIND54}} - \frac{\text{LIND93}}{\text{LIND54}}$ AFN=SS stored as DLIND55

SAM# DLIND56 - DLIND55 AFN=AS plotted

FIGURE 2. Subtractions in equation form

The second method involved subtracting the "wet" polymer (LIND55) from the "wet" protein coated polymer (LIND56), using the SSM command. With AFN=SS, the new "wet" protein spectrum was stored as a new file (NLIND56). In this step the water component of the two spectra should subtract out. There is, however, some residual water due to unequal quantities of water in the original samples. In order to complete the last step of the subtraction using the

SAM command, the single beam water vapor file had to be converted to an absorbance file by either ratioing it to the crystal or subtracting the crystal spectrum from it. With AFN=TS, this was stored as LIND193. Finally, by subtracting the water vapor (LIND193) from the "wet" protein (NLIND56) using the SAM command, only the "dry" protein remains. AFN is set to AS to plot the resulting spectrum. The subtractions described above are given in Figure 3 in equation form.

SSM#	$\frac{\text{LIND56}}{\text{LIND54}} - \frac{\text{LIND55}}{\text{LIND54}}$	AFN=SS	stored as NLIND56
	LIND93-LIND54	AFN=TS	stored as LIND193
SAM#	NLIND56 - LIND193	AFN=AS	plotted

FIGURE 3. Subtractions illustrated in equation form

Although both subtraction methods yielded identical results, the second method was chosen because it involved one less subtraction. Care must be taken when using the subtract programs as it is possible to artificially generate data.

Protein Spectra

To obtain protein ATR spectra, dilutions of albumin and fibrinogen were made at 50 mg/ml and 5 mg/ml, respectively. 0.06 ml of fibrinogen was carefully pipetted onto the germanium crystal and air dried. A spectrum was collected and stored. The crystal was thoroughly cleaned

before applying 0.06 ml of albumin. Again the crystal was air dried and a spectrum was collected.

Air Dried Silicone Rubber and Hydrogels

5x10 mm sections of silicone rubber, 5% HEMA/15% NVP on silicone rubber, 10% HEMA/10% NVP on silicone rubber, and 15% HEMA/5% NVP on silicone rubber were allowed to air dry. Spectra were collected, and then water vapor was subtracted using the same methods described above.

RESULTS AND DISCUSSION

Method 1

Blood Data- Method 1

As can be seen from Table 2, the first formulation inserted always remained patent for at least 45 minutes of exposure to flowing blood, the second remained patent twice and clotted once, the third remained patent once and clotted twice, and the fourth clotted each time. It was decided that recannulating the artery and vein four times was too traumatic for the vessels. Therefore, this method was abandoned.

SEM Results

Silicone rubber (dog 2959) in Figure 4a has a uniform distribution of platelets while Figure 4b, (also silicone rubber (dog 2913)) shows an uneven distribution of leucocytes. Figures 4c and 4d are micrographs of 5% HEMA/15% NVP (dog 2959) and represent adjacent areas on the same surface, while 5% HEMA/15% NVP (dog 2961) in Figure 4e shows a uniform distribution of platelets. Platelet degranulation products can be observed in Figures 4c, 4d, and 5a. Mostly white cells are attached to the 10% HEMA/10% NVP (dog 2959) surface in Figure 5a. Platelets uniformly cover the surface of 15% HEMA/5% NVP (dog 2961) in Figure 5b. Only those samples which remained patent for 45 minutes

TABLE 2. Data from Method 1

Dog Number	Formulation	Order of insertion	Platelet Number #/mm^3	Clot (min)	Patent (min)
2959			91,500		
	silicone rubber	1			45
	5% HEMA/ 15% NVP	3			45
	10% HEMA/ 10% NVP	2			45
	15% HEMA/ 5% NVP	4		30	
2913			405,000		
	silicone rubber	1			45
	5% HEMA/ 15% NVP	3		20	
	10% HEMA/ 10% NVP	4		33	
	15% HEMA/ 5% NVP	2		25	
2961			254,000		
	silicone rubber	4		25	
	5% HEMA/ 15% NVP	2			45
	10% HEMA/ 10% NVP	3		25	
	15% HEMA/ 5% NVP	1			45

are presented.

FT-IR Results

Figure 6 illustrates a representative silicone rubber IR spectrum from implantation Method 1. A very large peak is observed at 1258 wavenumbers and is believed to be a methyl vibration caused by deformation of the silicone rubber matrix when the tubing was flattened against the crystal. Sharp peaks often shift location in the spectrum by migrating a few wavenumbers in either direction. Such shifts in peak frequency make spectral subtraction impossible. In addition, the large 1258 cm^{-1} band interferes with the 1240 cm^{-1} band which is common to many proteins.

Method 2

Blood Data- Method 2

The blood data from Method 2 are presented in Table 3. These values are normal for healthy dogs.

Visual Observations

After flushing them with saline, the flowcells were observed macroscopically. There were no clots or erythrocytes visible in either flowcell from dog G.S. Examination of the flowcells used in dog 3172 also revealed no clots; however, there were erythrocytes on the surfaces.

FIGURE 4. Scanning electron micrographs of silicone rubber (A and B) and 5% HEMA/15% NVP (C, D, and E). 15 KeV. (scale bar=10 μm)

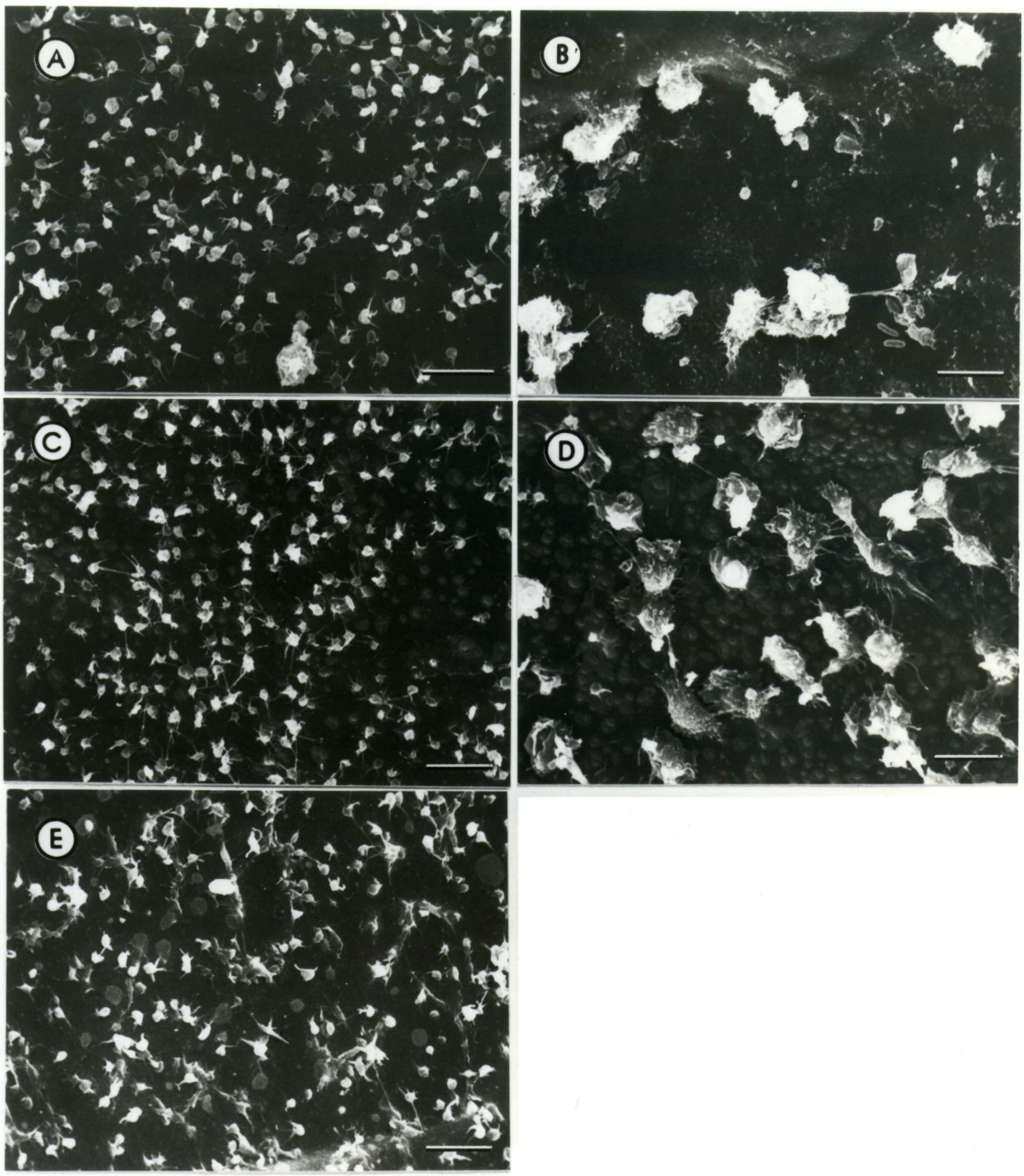
A
B
C
D
E

FIGURE 5. Scanning electron micrographs of 10% HEMA/10% NVP (A) and 15% HEMA/5% NVP (B). 15 KeV. (scale bar=10 μm)

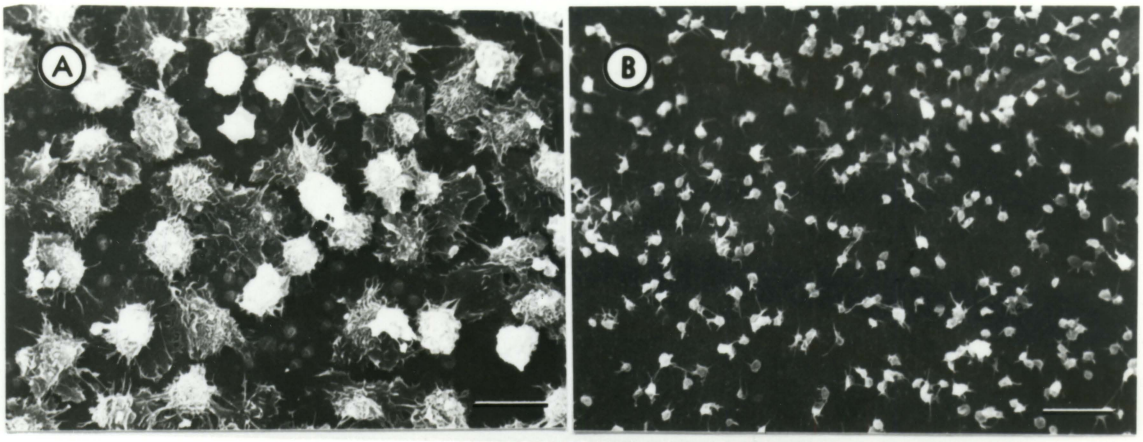
A
B

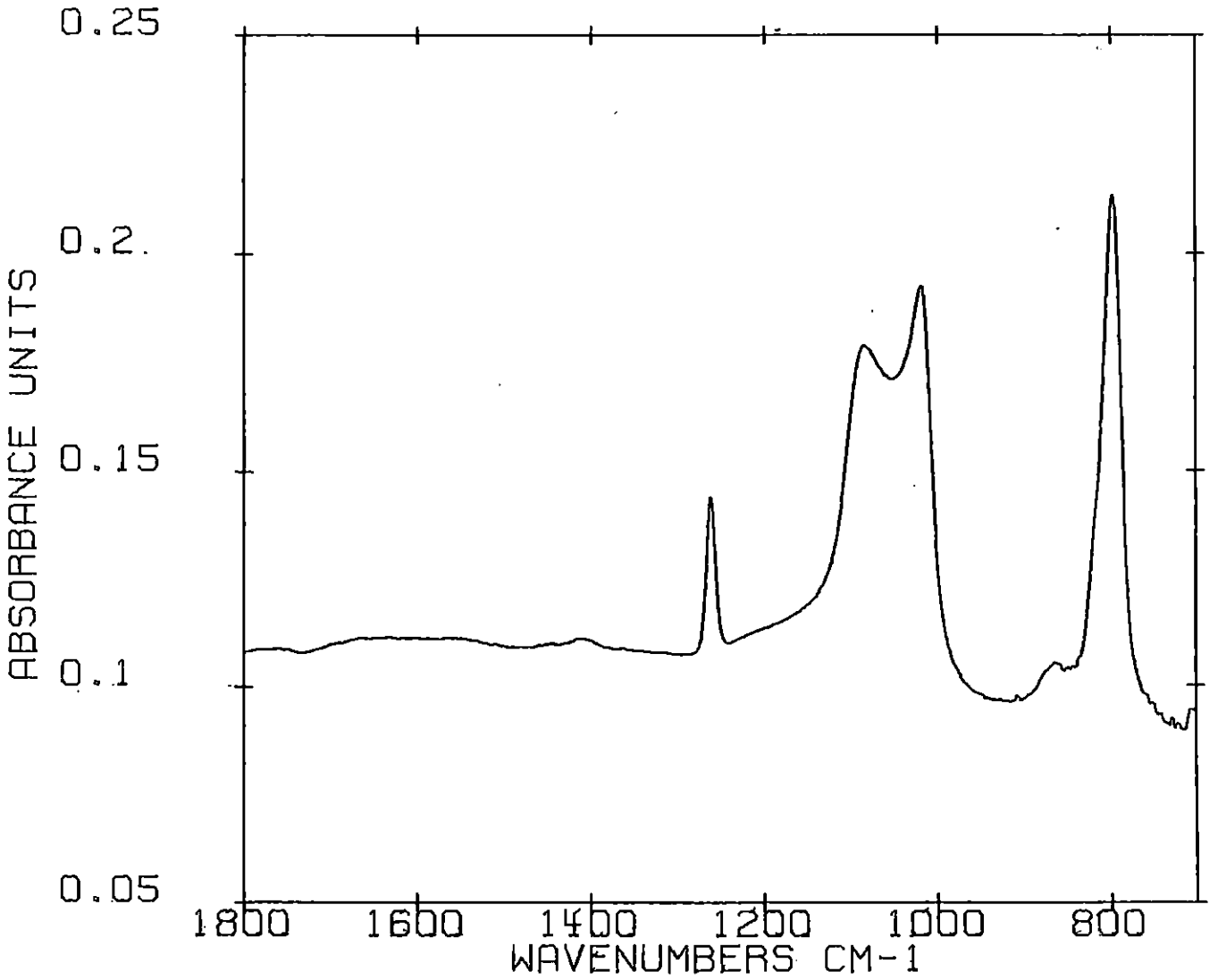

FIGURE 6. Spectrum of silicone rubber tubing showing large peak at 1258 wavenumbers

TABLE 3. Data from Method 2

Dog Number	Platelet Count #/mm³	ACT (sec)
G.S.	NA	NA
3172	254,000	80
3178	186,000	85

In particular, silicone rubber from both flowcells and 10% HEMA/10% NVP from the right flowcell appeared to have larger deposits of erythrocytes than the other surfaces from the same dog. While examining the right flowcell from dog 3178, a thin sheetlike film of erythrocytes and fibrin was noticed on the silicone rubber, and this also hung from the open end of the flowcell. The effect of the silicone rubber appeared to have spread to the adjacent sample, 5% HEMA/15% NVP, by covering half of it with the same red cell fibrin film. In an attempt to remove the excess fibrin, some of the deposit on the silicone rubber was accidently stripped away. The left leg assembly was also grossly coated with the red cell fibrin film. It is believed that the coating on the inside of the syringes was not thoroughly removed prior to coating the inside with silicone rubber.

SEM Results

Figures 7a through 12e are SEM micrographs illustrating the blood's response to surfaces varying in hydrophilicity. Some of the red cells found in the following SEM micrographs are crenated as in Figure 7a. This is believed to be a fixation artifact. Compare the crenated cells of Figure 7a with the normal cells in Figure 7b. A diversified response is seen in Figures 7a to 8d (dog 3178). An extensive network of fibrin with entrapped erythrocytes is observed on silicone rubber (Figure 7a) and 5% HEMA/15% NVP (Figures 7b and 7c), while a large thrombus with entrapped white cells is seen on another area of 5% HEMA/15% NVP (Figure 7d). The reaction to 10% HEMA/10% NVP ranges from areas of complete fibrin cover with some formed elements (Figures 7e and 7f) to areas with predominantly leucocytes and almost no fibrin (Figure 8a). Note the uniform alignment of the fibrin strands in Figure 7e. The reaction to 15% HEMA/5% NVP also ranges from an extensive fibrin network (Figures 8b and 8c) in some areas to minimal deposition in others (Figure 8d).

The reaction to the test surfaces was again observed when they were implanted in dog G.S. (Figures 9a through 10c). The silicone rubber surface (Figures 9a and 9b) attracted many erythrocytes with some fibrin in some areas and only a few cellular elements in others. The reaction to 5% HEMA/15% NVP (Figures 9c and 9d) was similar to that of

FIGURE 7. Scanning electron micrographs of silicone rubber (A), 5% HEMA/15% NVP (B, C, and D), and 10% HEMA/10% NVP (E and F). 15 KeV. (scale bar=10 μm)

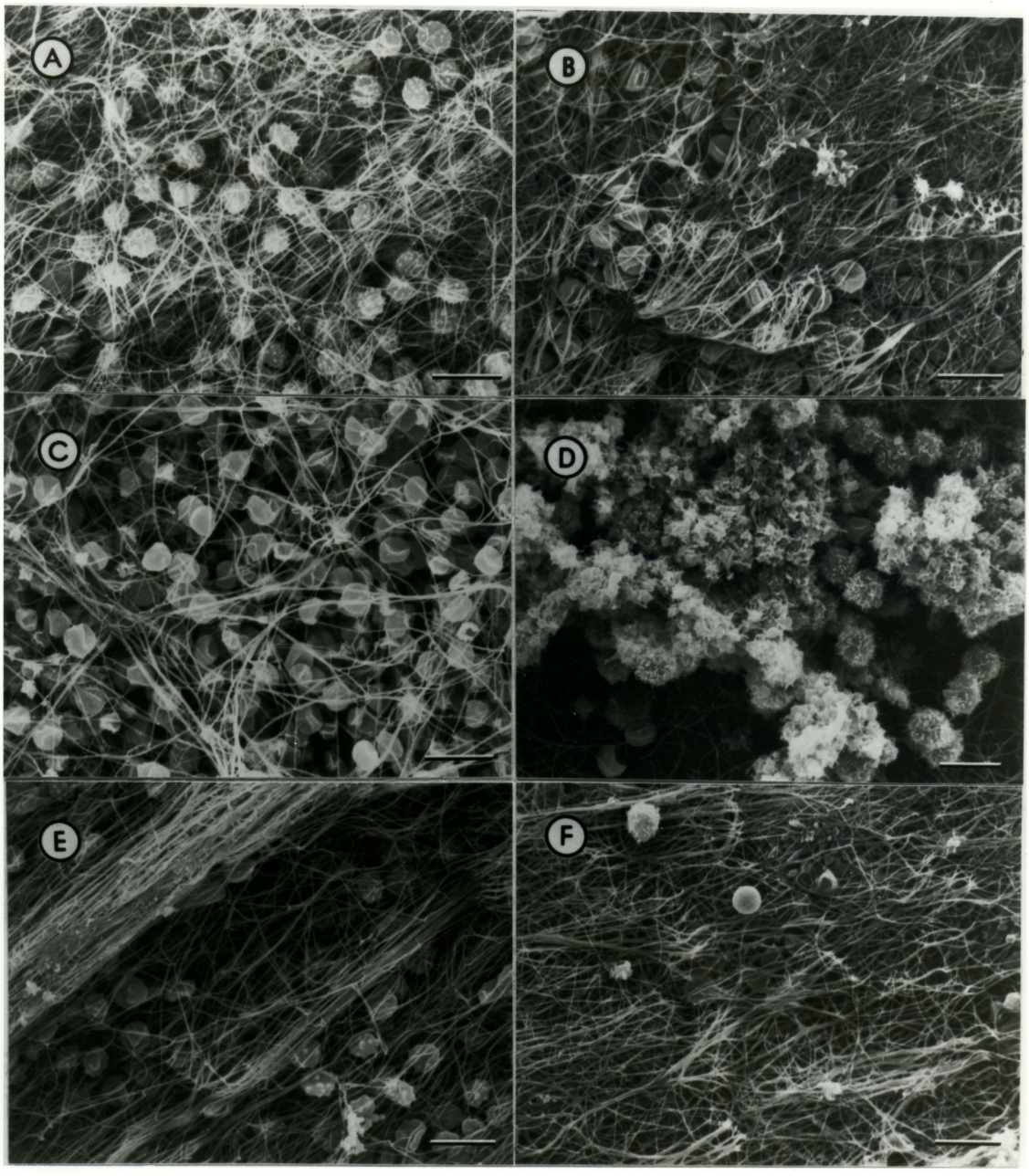
A
B
C
D
E
F

FIGURE 8. Scanning electron micrographs of 10% HEMA/10% NVP (A) and 15% HEMA/5% NVP (B, C, and D). 15 Kev. (scale bar=10 μm)

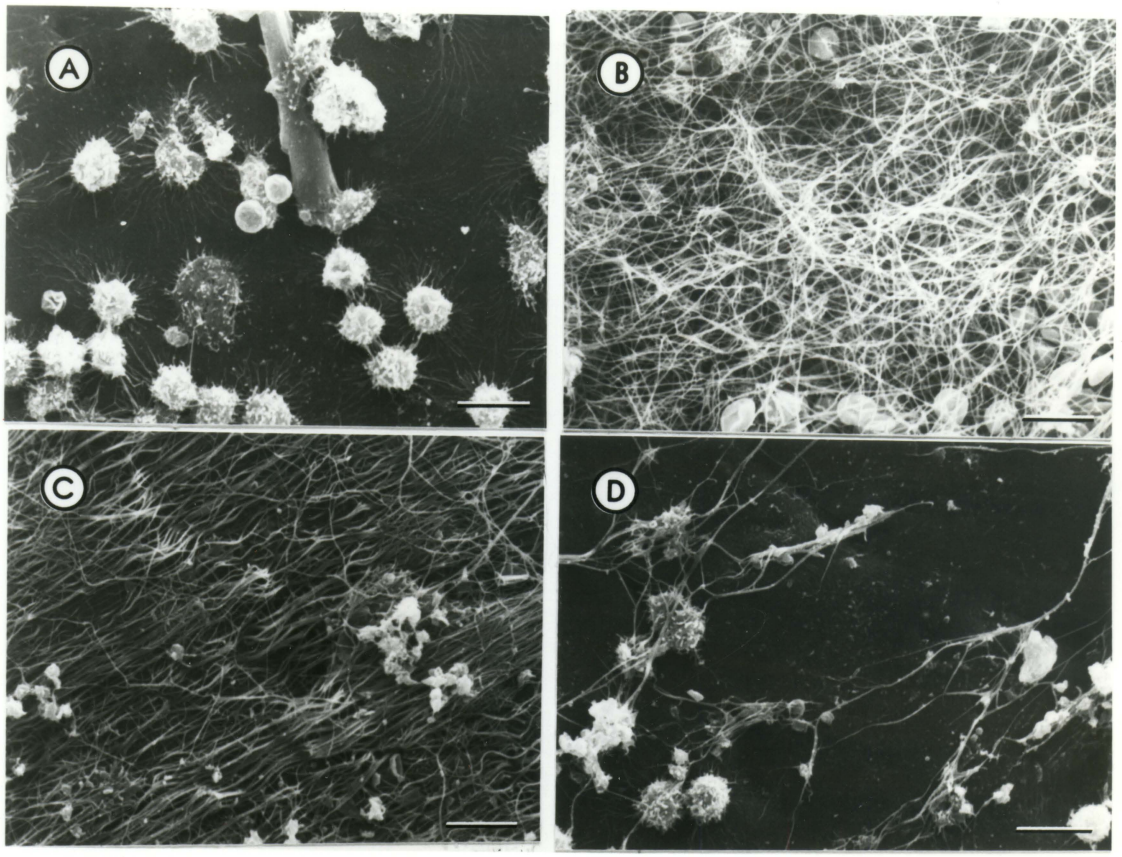
A
B
C
D

silicone rubber, but the surface attracted more fibrin than erythrocytes. A few leucocytes are seen on Figure 9. Figure 9c also shows a few platelet clumps. Almost no fibrin is present on the 10% HEMA/10% NVP (Figure 10a) and 15% HEMA/5% NVP surfaces (Figures 10b and 10c), but varying quantities of platelets and white cells are attached.

The response of dog 3172 to the test materials is illustrated in Figures 11a through 12e. The deposition onto this silicone rubber (Figure 11a) surface appeared to occur in streaks. The direction of flow was perpendicular to the streaks. At higher magnification (Figure 11b) the light areas are seen to be primarily erythrocytes and fibrin while the dark areas (Figure 11c) have only a few adherent platelets. Deposition onto 5% HEMA/15% NVP ranged from areas of extensive fibrin (Figure 11d) to areas with only a few white cells (Figure 11e). Note the development of pseudopods on the platelets. Mostly erythrocytes and fibrin were attracted to the 10% HEMA/10% NVP surface (Figures 12a to 12c). A cluster of platelets can be observed in the center of Figure 12c. The 15% HEMA/5% NVP surface (Figures 12d and 12e) attracted the least fibrin, and the adherent formed elements range from primarily platelets to a few white cells.

Overall, the least material adhered to the 15% HEMA/5% NVP surface. Although some of the 15% HEMA/5% NVP surfaces

FIGURE 9. Scanning electron micrographs of silicone rubber (A and B) and 5% HEMA/15% NVP (C and D). 15 Kev. (scale bar=10 μm)

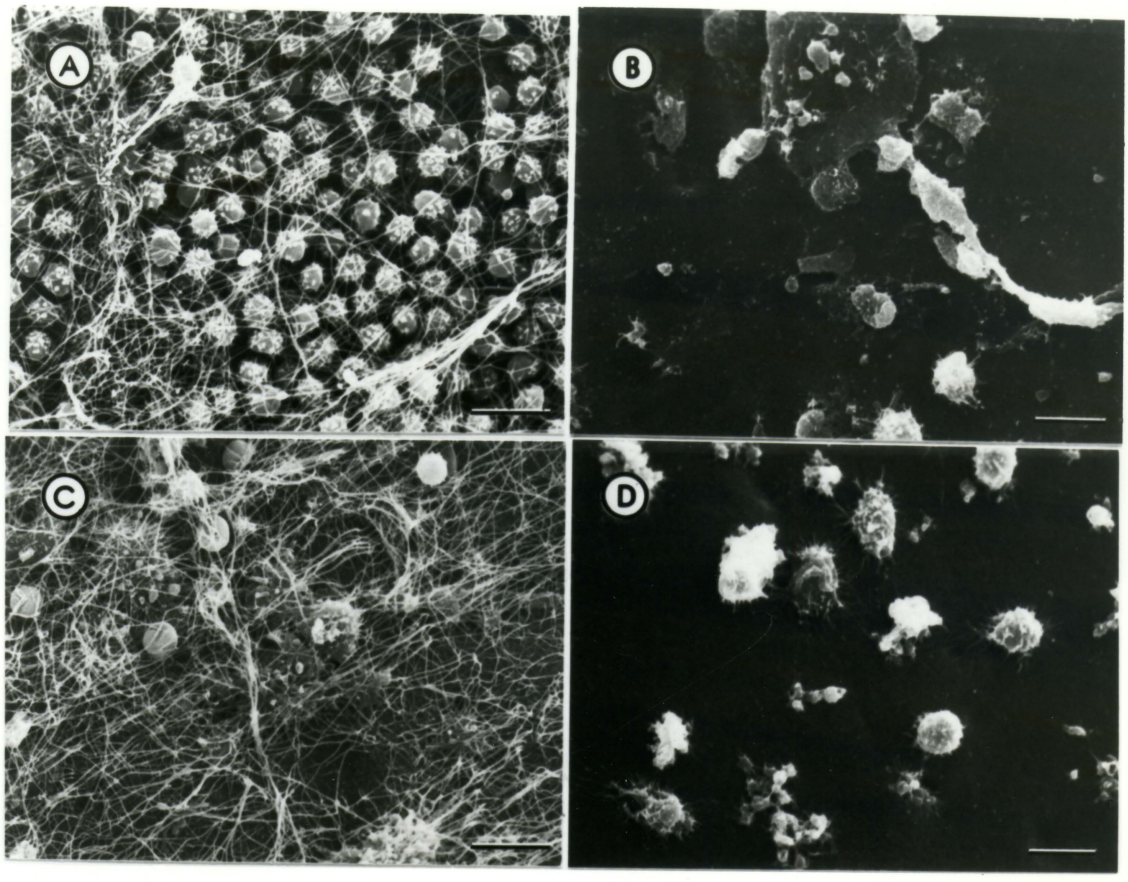
A
B
C
D

FIGURE 10. Scanning electron micrographs of 10% HEMA/10% NVP (A) and 15% HEMA/5% NVP (B and C). 15 Kev. (scale bar=10 μm)

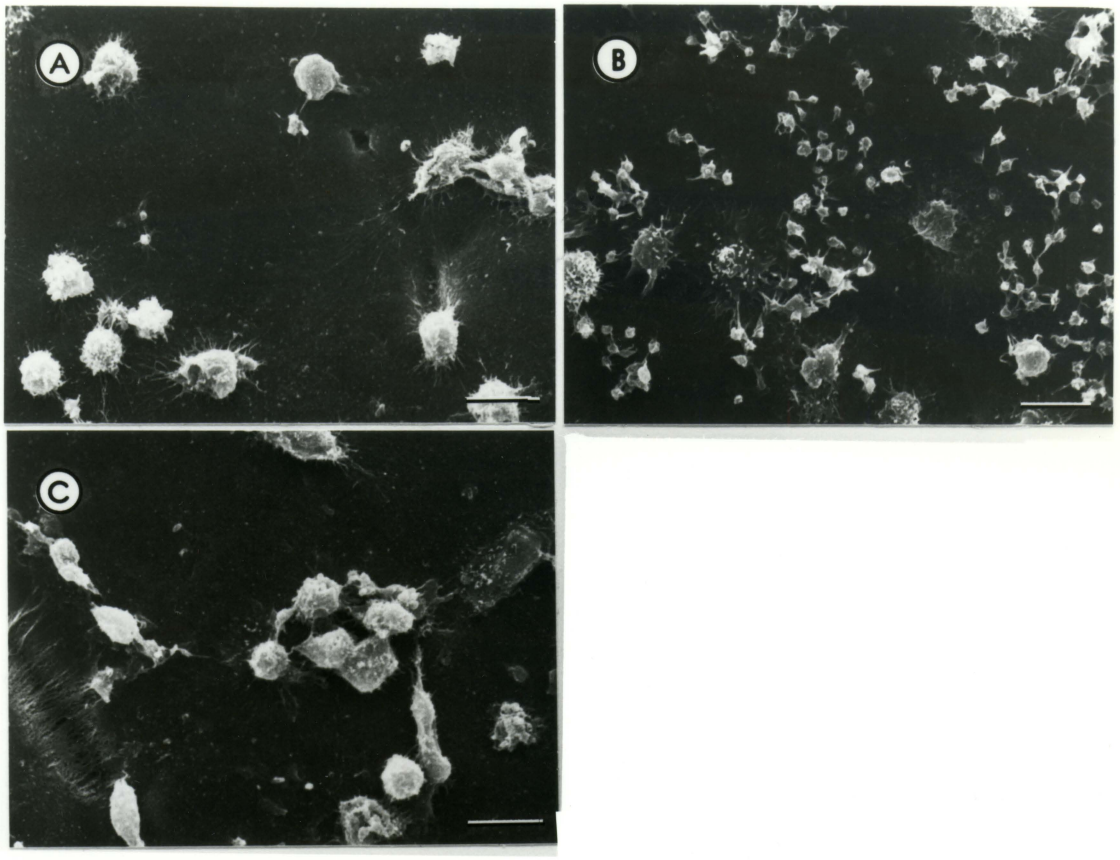
A
B
C

FIGURE 11. Scanning electron micrographs of silicone rubber (A, B, and C) and 5% HEMA/15% NVP (D and E). 15 Kev. (scale bar A =250 μm, scale bar B, C, D, E =10 μm)

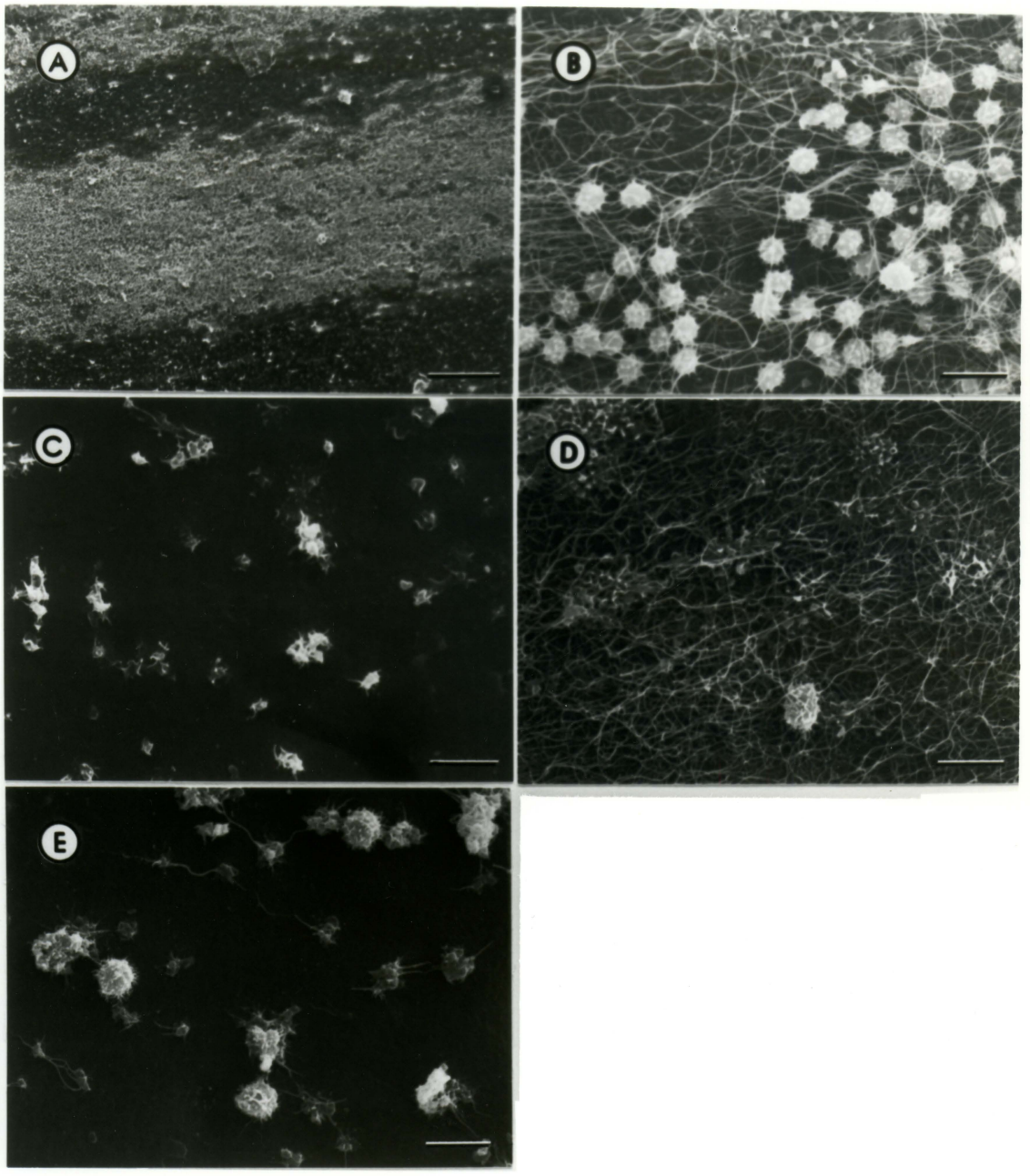
A
B
C
D
E

FIGURE 12. Scanning electron micrographs of 10% HEMA/10% NVP (A, B, and C) and 15% HEMA/5% NVP (D and E). 15 KeV. (scale bar A=33.3 μm, scale bar B, C, D, E=10 μm)

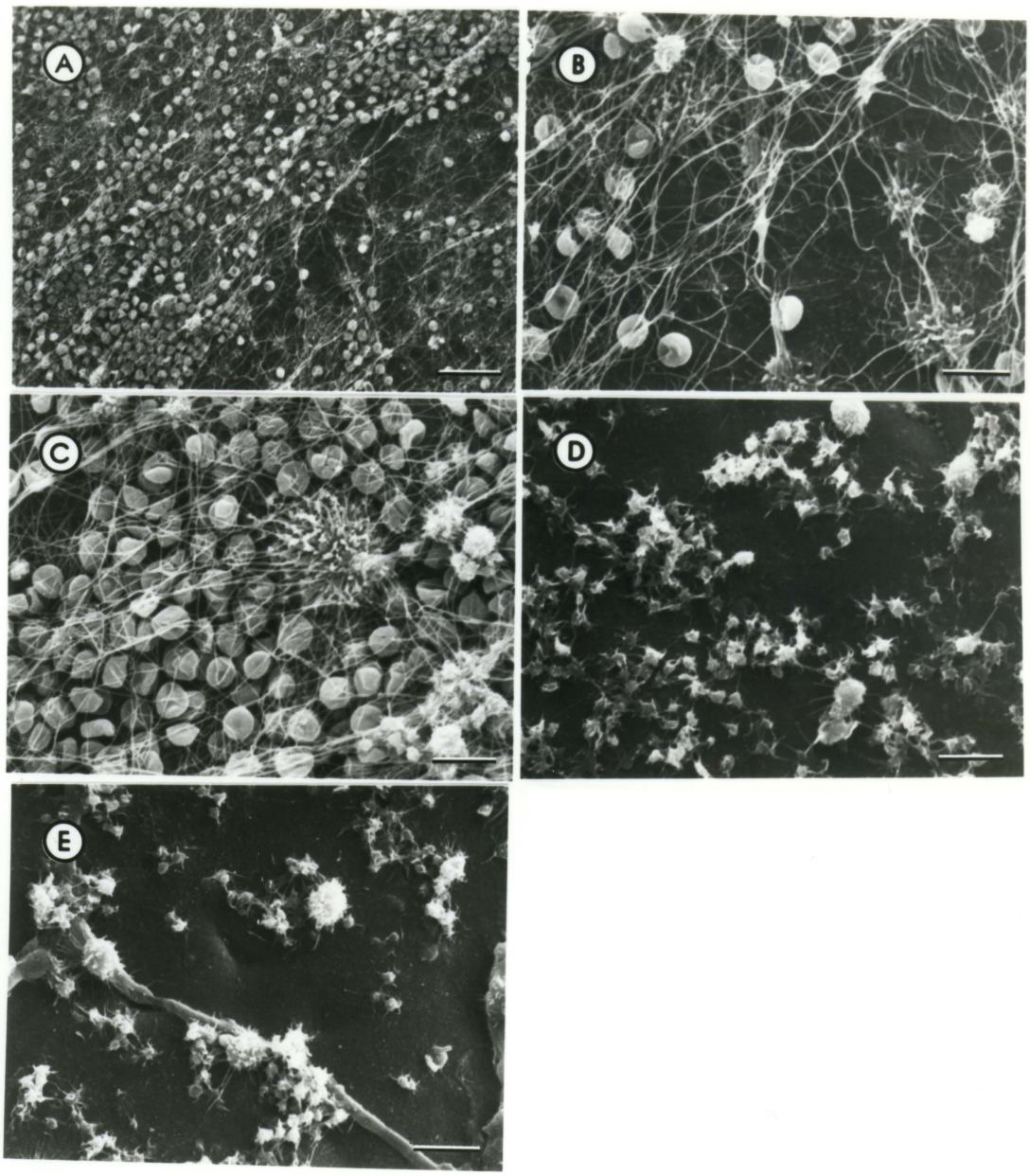
A
B
C
D
E

were heavily covered with fibrin, more fibrin was found on the silicone rubber surfaces. However, some regions of the silicone rubber surfaces were clean, and large fibrin and red cell deposits were also found on each of the other surfaces. In general, the silicone rubber surfaces were more heavily covered with fibrin and cellular elements than the hydrogel grafted samples. The reactions observed are believed to be the result of decreased adhesion to the hydrophilic hydrogel samples compared with silicone rubber. In general, the greater the degree of hydrophilicity of the hydrogel, the less material was observed to be adsorbed after the 15 minute exposure (i.e., 15% HEMA/5% NVP and 10% HEMA/10% NVP compared with the 5% HEMA/15% NVP samples).

FT-IR Results

The spectra collected during the FT-IR experiments are presented in Figures 13 to 22.

Figure 13 shows the ratio of two germanium spectra that were collected during the alignment experiment. The resulting curve is almost a straight line and indicates that the two original spectra were nearly identical.

The next two spectra (Figure 14) represent the result of applying silicone rubber strips to the germanium crystal with varying degrees of pressure. The upper spectrum (A) was obtained using relatively low pressure while the lower spectrum (B) was obtained using relatively high pressure.

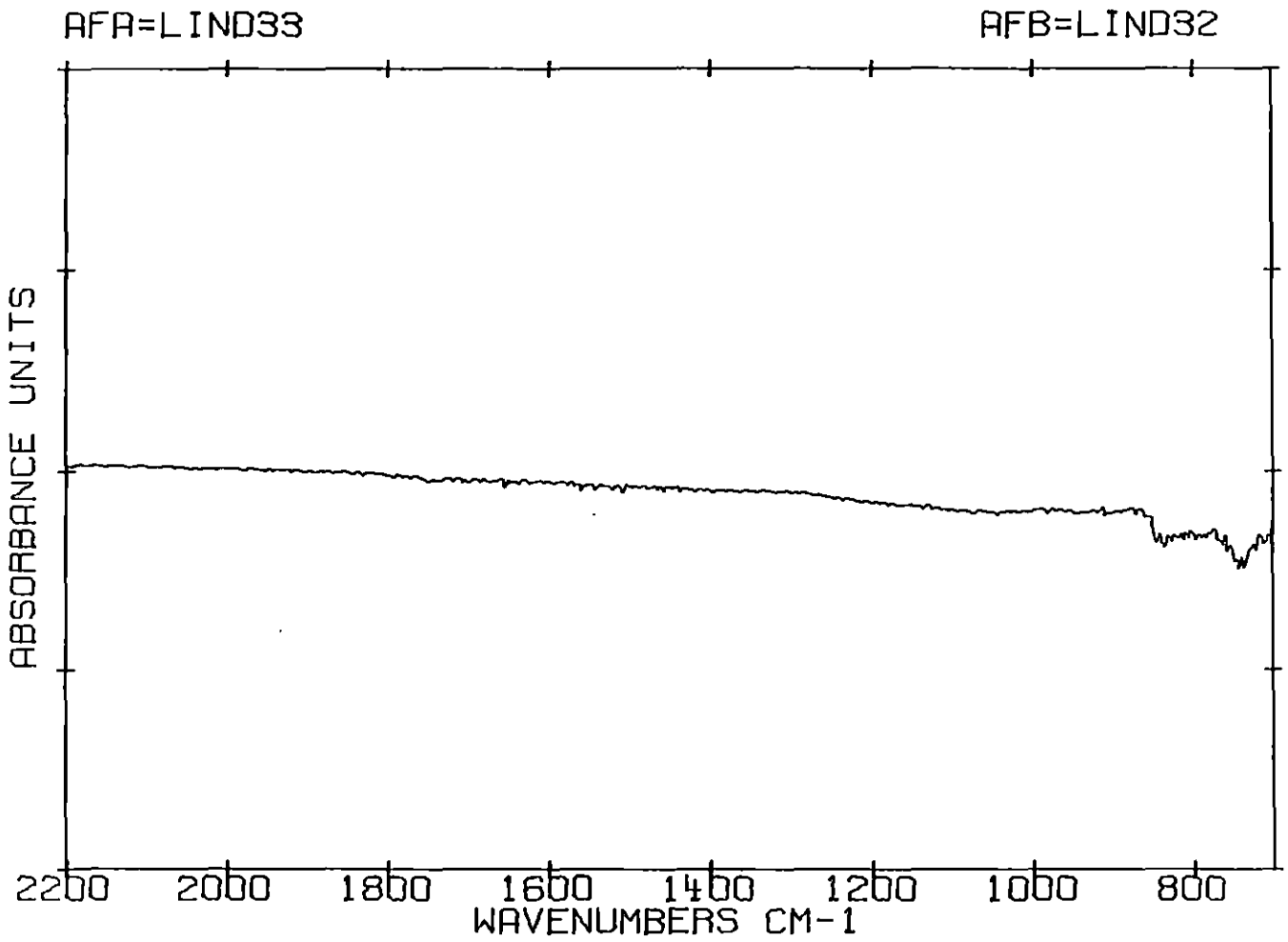

FIGURE 13. Comparison of two germanium spectra collected during alignment experiment

Note the increase in intensity of the 1258, 1013, and 793 cm^{-1} silicone rubber bands in (B).

When performing the subtractions (see Appendix C), one peak is monitored. The peak chosen should exist in the reference spectrum, but not in the sample spectrum. The subtraction continues until the peak disappears. In some instances, the peak cannot be completely subtracted and a dispersion curve results. Part of the peak is above and part below the spectrum as indicated by the arrow in Figure 15 which was obtained by subtracting a spectrum of water vapor from the spectrum of protein coated 5% HEMA/15% NVP. Dispersion curves are observed when an interaction occurs that shifts the peak a few wavenumbers. For example, if silicone rubber is subtracted from hydrogel coated silicone rubber and a dispersion curve results when trying to subtract a particular peak, then the hydrogel has reacted with the silicone rubber causing a frequency shift in the silicone rubber bands.

The next series of spectra (Figures 16 to 19) is representative of those collected for implantation Method 2. In all the figures, the upper spectrum is the single beam file ratioed to the crystal. This creates an absorbance file. No single beam files are presented. The lower spectra have the spectra of the appropriate polymers subtracted, leaving only the protein spectra.

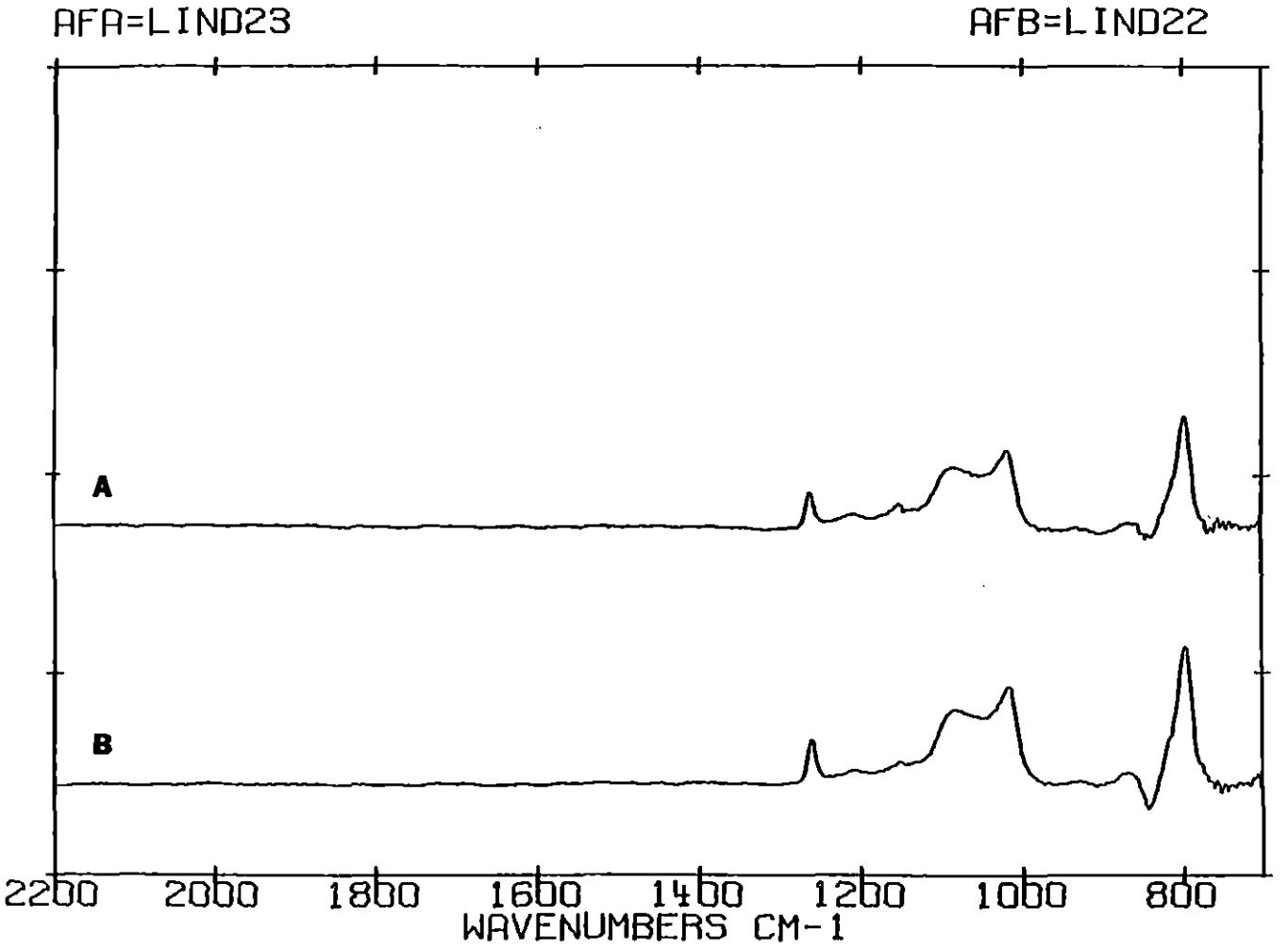

FIGURE 14. Spectra resulting from applying silicone rubber sheets to the crystal with varying degrees of pressure, upper spectrum (A) was collected using relatively less pressure than lower spectrum (B)

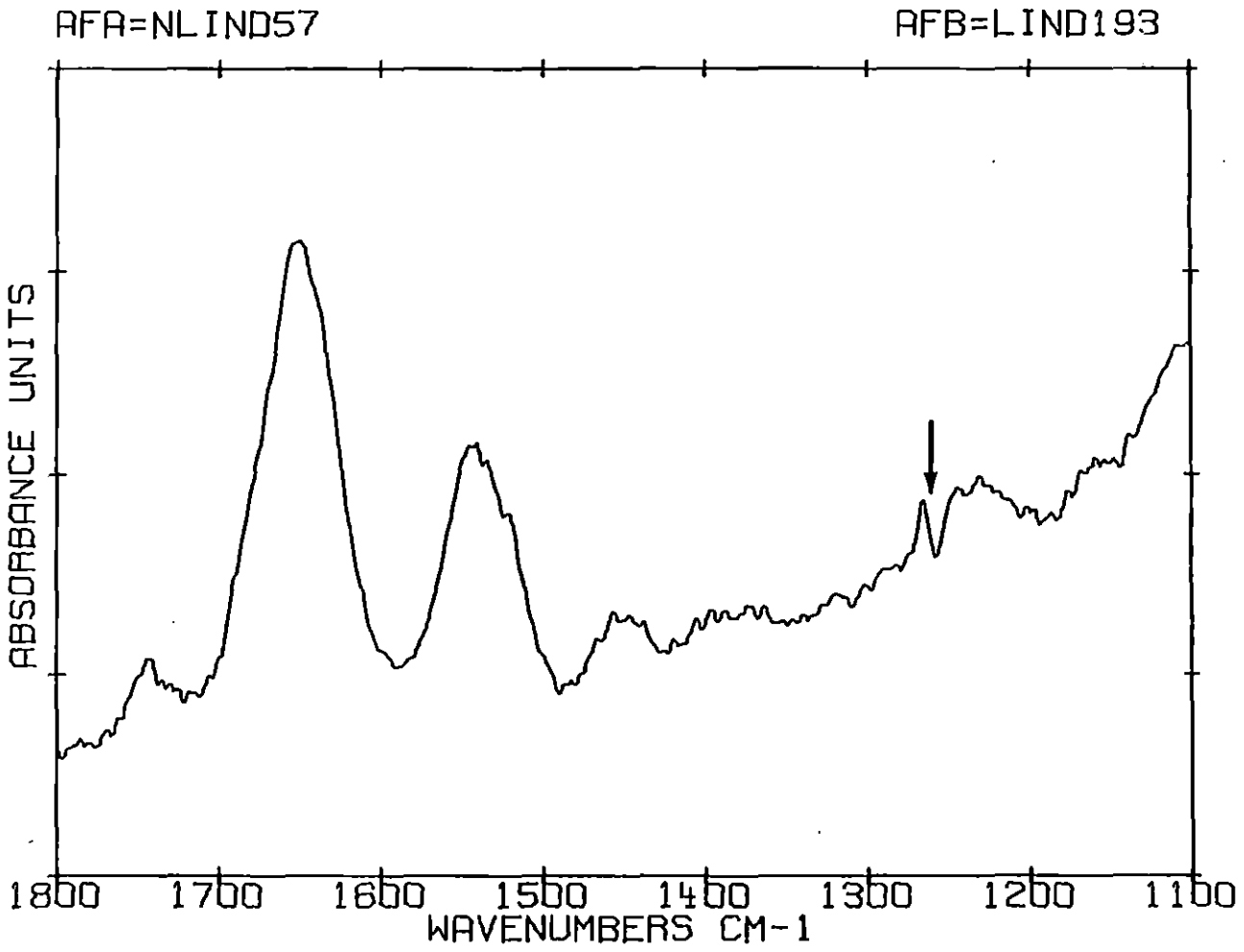

FIGURE 15. Spectrum of 5% HEMA/15% NVP after exposure to blood illustrating dispersion curves indicated by arrow

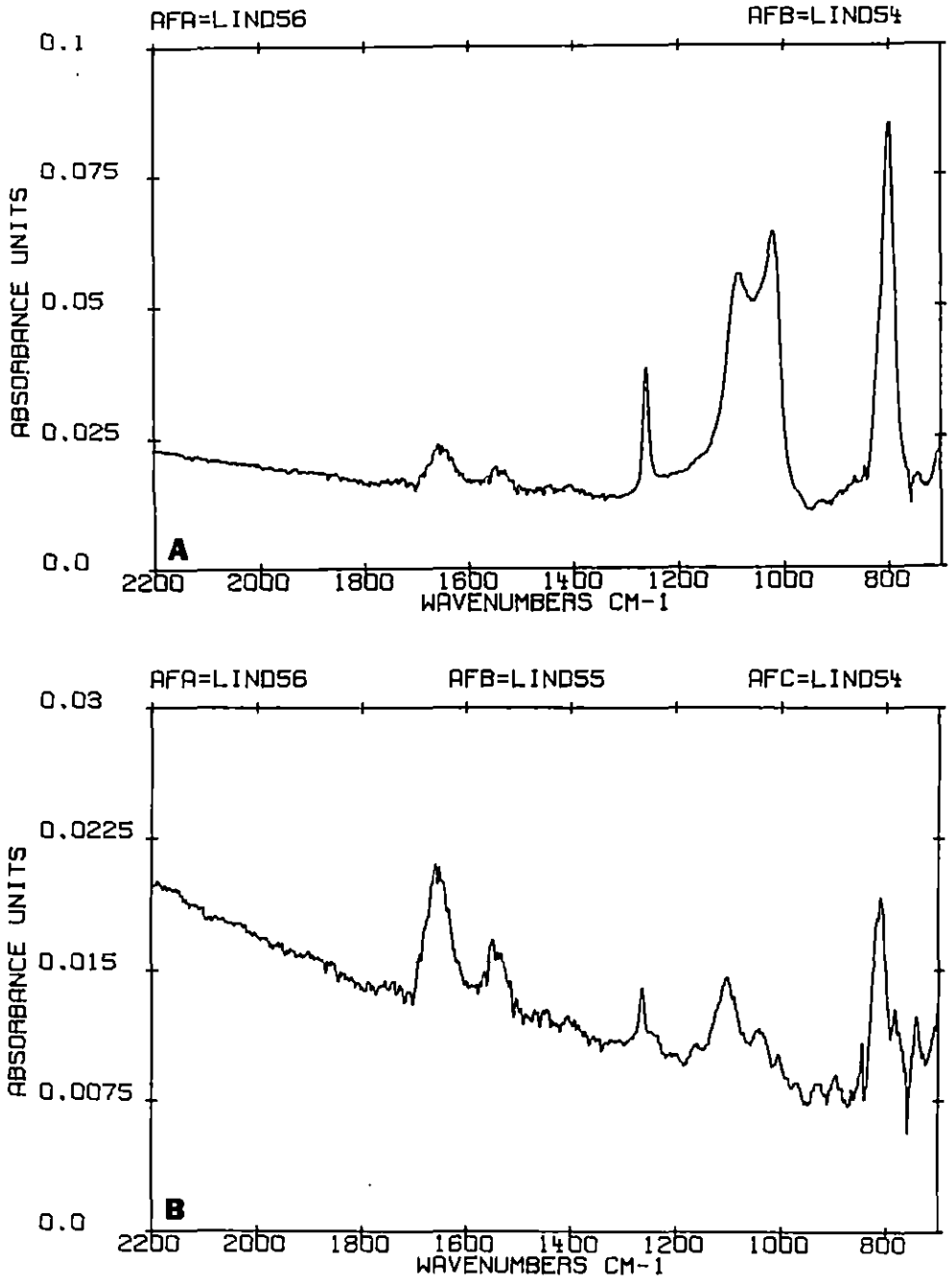

FIGURE 16. Absorbance spectra of silicone rubber after 15 minutes exposure to blood (A) and the protein layer after silicone rubber subtraction (B)

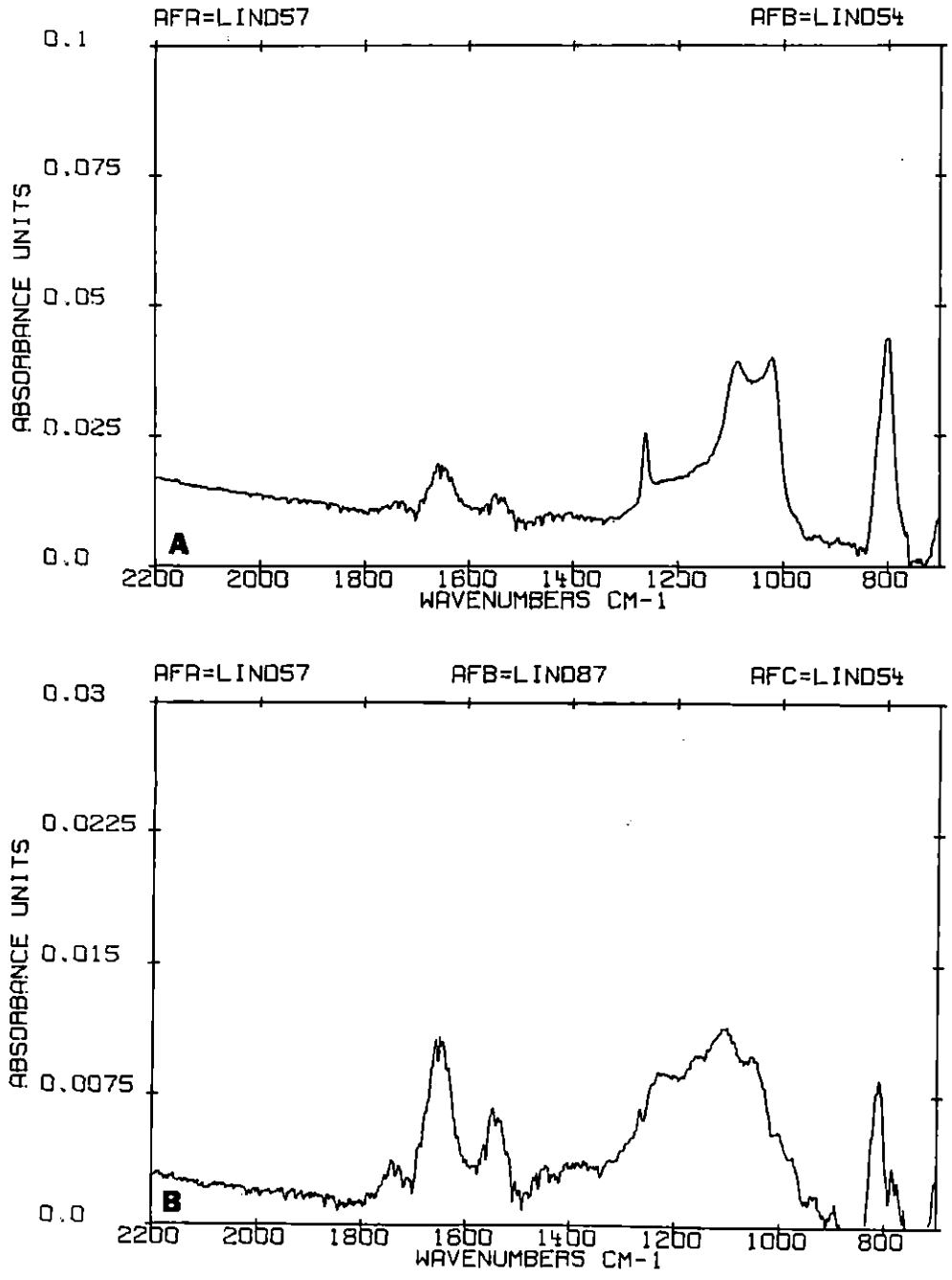

FIGURE 17. Absorbance spectra of 5% HEMA/15% NVP after 15 minutes exposure to blood (A) and the protein layer after subtraction of the 5% HEMA/15% NVP (B)

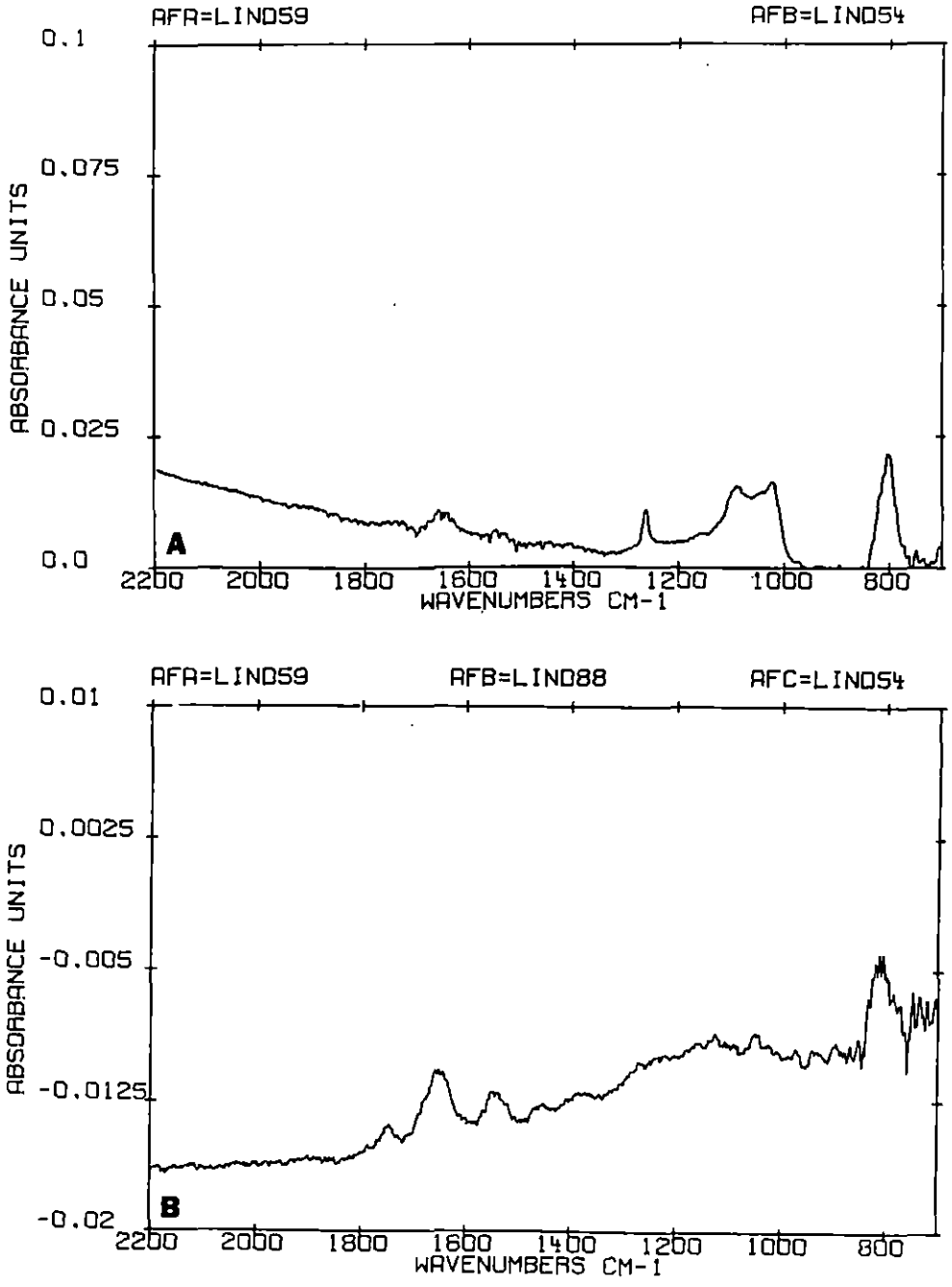

FIGURE 18. Absorbance spectra of 10% HEMA/10% NVP after 15 minutes exposure to blood (A) and the protein layer after subtraction of the 10% HEMA/10% NVP (B)

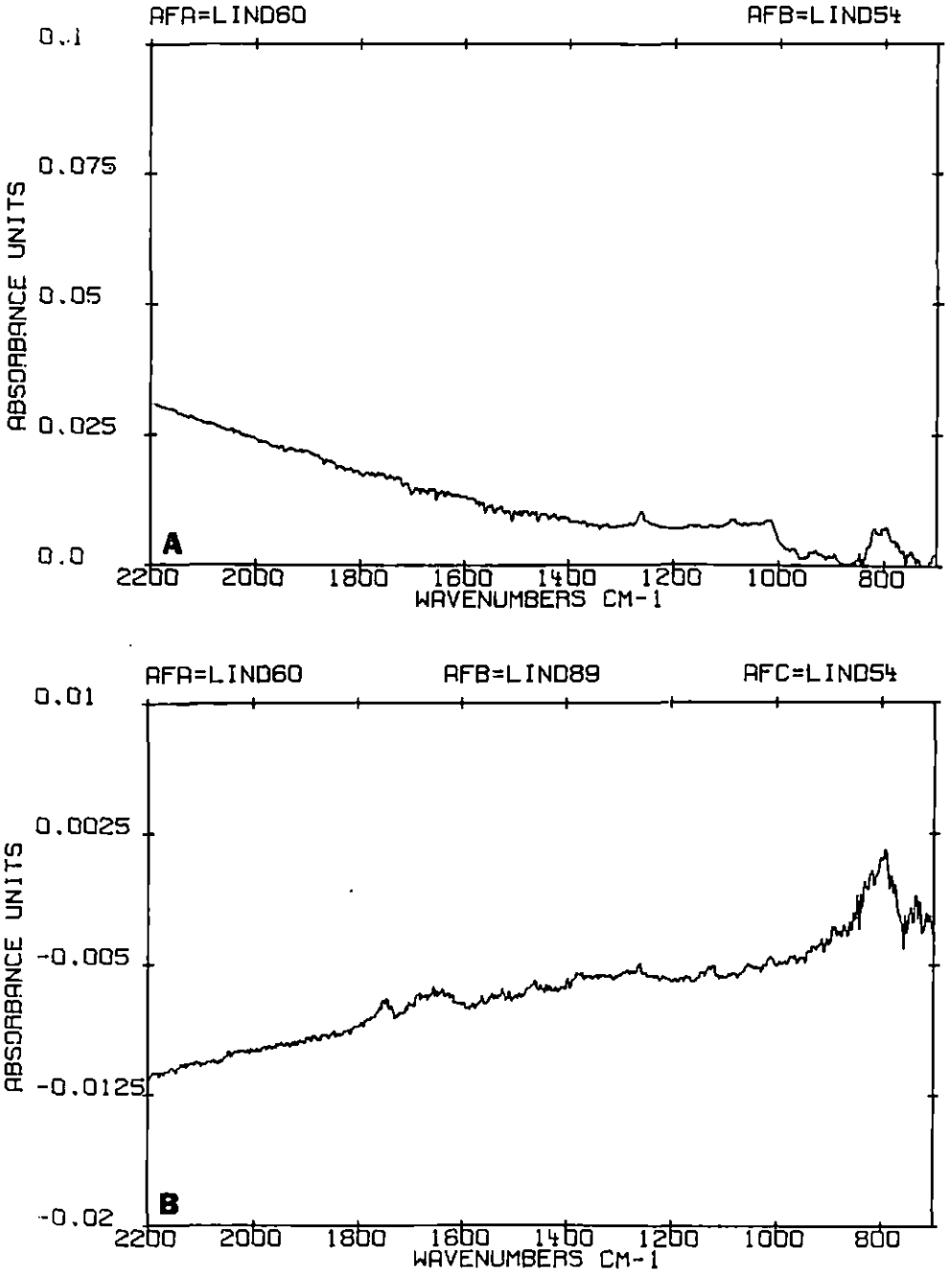

FIGURE 19. Absorbance spectra of 15% HEMA/5% NVP after 15 minutes exposure to blood (A) and the protein layer after subtraction of the 15% HEMA/5% NVP (B)

To determine the relative quantity of protein on each surface based on the FT-IR spectra, the spectra were rated and ranked. Because the 1650 and 1550 cm^{-1} bands are common to all plasma proteins, these bands were used to rate the spectra. Within a group composed of silicone rubber, 5% HEMA/15% NVP, 10% HEMA/10% NVP, and 15% HEMA/5% NVP, the spectrum with the most protein was rated a 4, the next lower a 3, etc. The ratings were always started with the spectrum having the largest peaks and progressed to those having the smallest. If two spectra could not be differentiated, they were scored equally. The results of the ratings are presented in Table 4. The ratings were totalled for a final comparison. Note that within the hydrogel coated samples, 15% HEMA/5% NVP had the lowest protein deposits compared with 10% HEMA/10% NVP (intermediate) and 5% HEMA/15% NVP (the most). Also, the amount of protein on the 15% HEMA/5% NVP formulation was somewhat lower than for silicone rubber. Within a formulation type for any particular dog, usually less protein was seen deposited for samples initially exposed (i.e., right leg, initial insertion, compared with left leg, latter insertion).

For reference purposes, the water vapor spectrum that was used in the water subtractions described in the Methods section is presented in Figure 20. As previously mentioned, the two methods of water subtraction yielded identical

TABLE 4. Ratings of Protein Spectra

Dog number	S.R.*	5% H/15% N	10% H/10% N	15% H/5% N
G.S. (right)	3	4	2	1
G.S. (left)	4	4	3	2
3172 (right)	1	4	3	2
3172 (left)	2	4	3	1
3178 (right)	1	4	3	2
3178 (left)	2	3	4	2
Total	13	23	18	10

*S.R.=silicone rubber, H=HEMA, N=NVP

spectra. These are illustrated in Figure 21 with the spectrum resulting from subtraction method 1 shown vertically displaced (i.e., subtraction method 1 results in A, subtraction method 2 results in B).

The spectra collected after drying single protein solutions onto the germanium crystal are presented in Figure 22. The upper spectrum is an absorbance spectrum created by ratioing fibrinogen to the crystal. The lower spectrum is an absorbance spectrum of albumin. The fibrinogen spectrum has a peak at 1580 wavenumbers, which is not found in the albumin spectrum, a much larger 1400 cm^{-1} band than in albumin, a trace of a 1240 cm^{-1} band, and slight evidence of a 1080 cm^{-1} band. The albumin spectrum has a small 1450

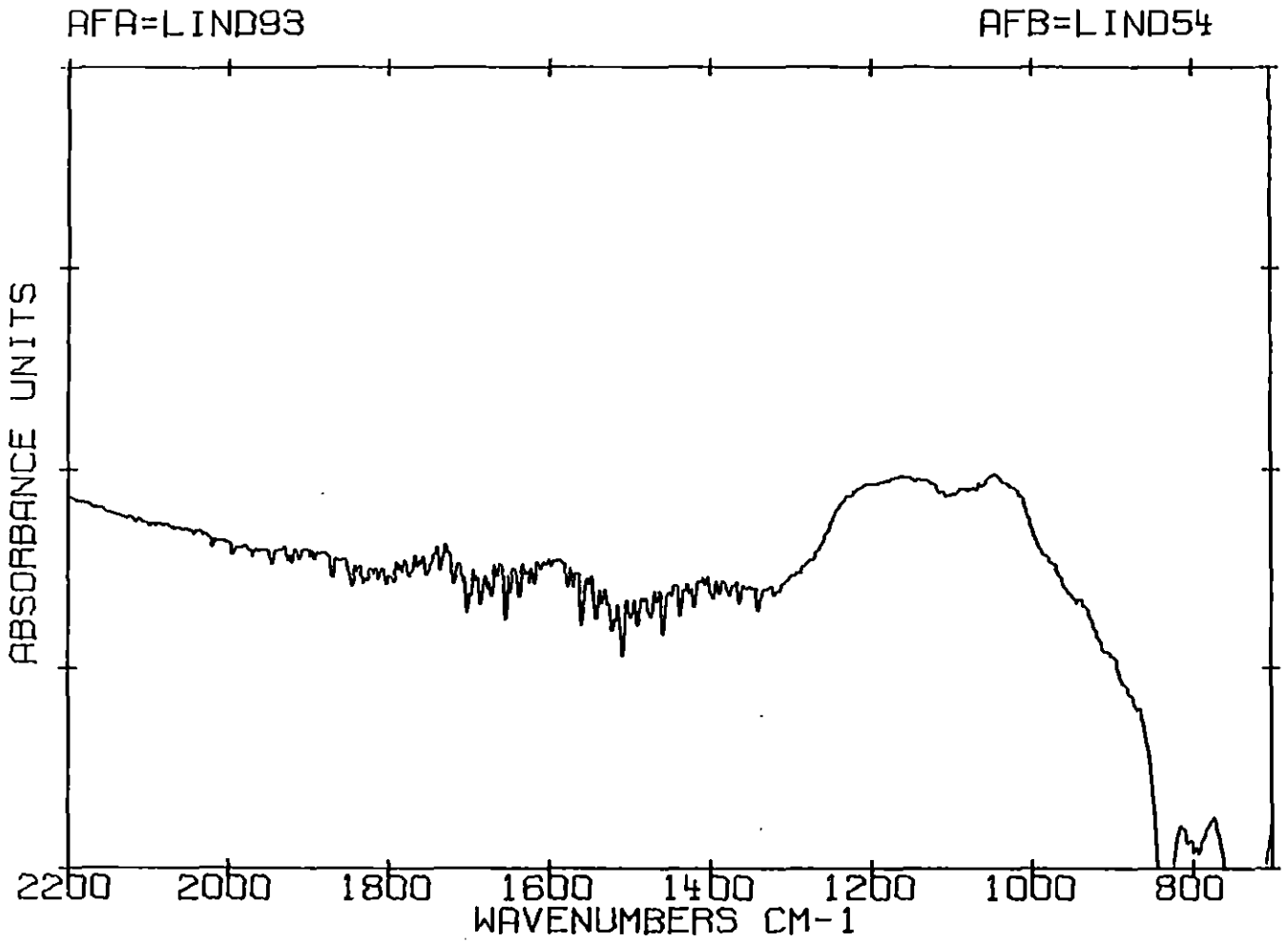

FIGURE 20. Absorbance spectrum of water vapor

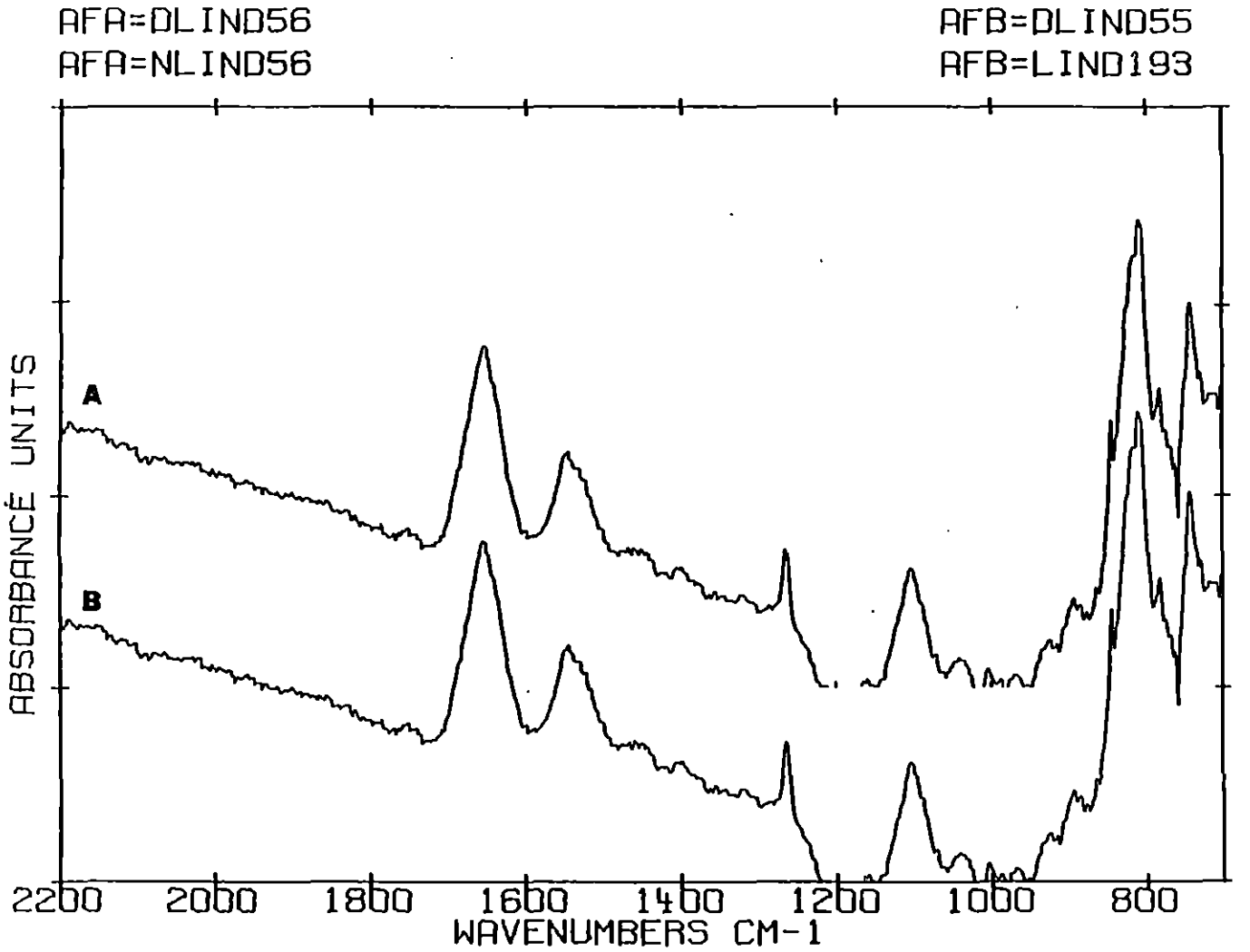

FIGURE 21. Comparison of spectra resulting from water subtractions, the upper spectrum (A) was obtained by method 1 and the lower spectrum (B) by method 2

cm^{-1} band where the same band in fibrinogen appears as a shoulder on the larger 1400 cm^{-1} peak. By comparison, the albumin spectrum has almost no 1240 cm^{-1} band.

Effect of Hydrogel Coating

Figure 23 illustrates the effect of radiation grafting HEMA and NVP onto silicone rubber sheeting. All original spectra were plotted on the same vertical scale. They are shown here vertically displaced for illustration purposes only. An absorption spectrum of silicone rubber is represented by spectrum A. Note the heights of the silicone rubber peaks at 1258, 1018, and 793 wavenumbers. When the silicone rubber was grafted with 5% HEMA/15% NVP, a large decrease in the silicone rubber peak intensities is observed (spectrum B). As the concentration of HEMA is increased in 10% HEMA/10% NVP (spectrum C), and in 15% HEMA/5% NVP (spectrum D) the silicone rubber peaks become masked even more. This corresponds to an increase in polymer grafted to the silicone rubber and is characterized and described in Vale and Greer (ca. 1982).

The spectra presented in Figures 24 and 25 represent air dried silicone rubber (Figure 24a), 5% HEMA/15% NVP (Figure 24b), 10% HEMA/10% NVP (Figure 25a), and 15% HEMA/5% NVP (Figure 25b). Although the sections were dried for equal times, the spectra show increasing quantities of water. All spectra had water vapor subtracted from them.

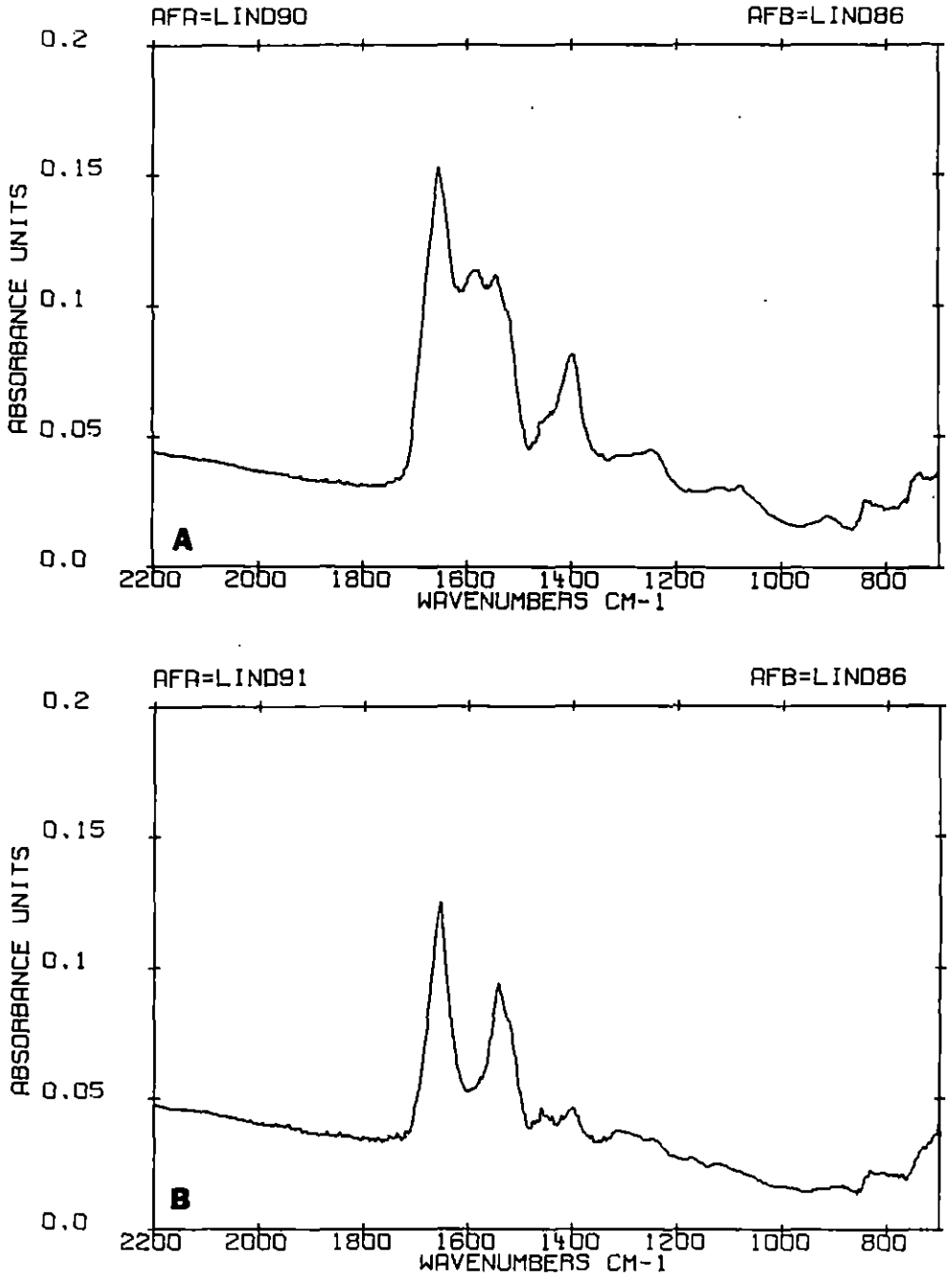

FIGURE 22. Absorbance spectra of fibrinogen (A) and albumin (B)

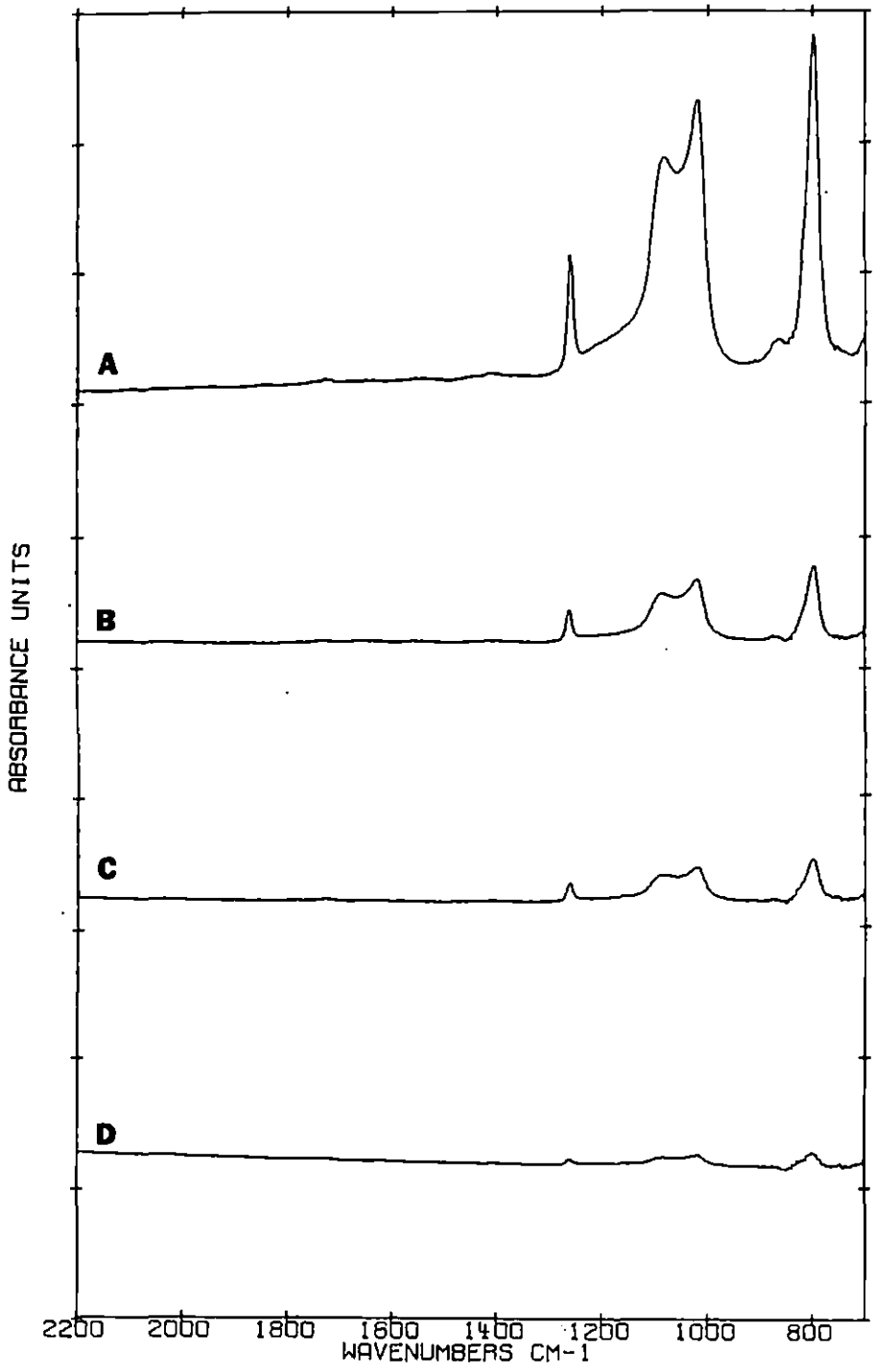

FIGURE 23. Absorbance spectra illustrating the effect of grafting HEMA and NVP onto silicone rubber, silicone rubber (A), 5% HEMA/15% NVP (B), 10% HEMA/10% NVP (C), and 15% HEMA/5% NVP (D)

The water under consideration is that which remains after the water vapor subtractions. The area of interest is between 1400 and 1800 wavenumbers. Silicone rubber (Figure 24a) retains almost no water. 5% HEMA/15% NVP (Figure 24b) retains more, as indicated by the very small amplitude, high frequency peaks between 1400 and 1800 wavenumbers. The high frequency water peaks become more evident in 10% HEMA/10% NVP (Figure 25a) and still more prominant in 15% HEMA/5% NVP (Figure 25b). The primary difference between Figures 23, 24, and 25 is that the samples in Figure 23 were more thoroughly dried.

FT-IR and SEM Results

In each case, Figures 26 to 28 show FT-IR spectra on the left with the SEM micrographs from the corresponding samples on the right. The FT-IR spectra and associated SEM micrograph(s) are arranged for any particular figure in the sequence: silicone rubber, 5% HEMA/15% NVP, 10% HEMA/10% NVP, 15% HEMA/5% NVP. Each figure contains the spectra and micrographs for the four test samples for a particular dog. FT-IR and SEM data are presented in two groupings: first, second implant series (left leg), and second, initial implant series (right leg). Comparisons can therefore be made of the amount of protein deposited for each sample type, for a dog, based on relative intensities of the protein peaks at 1650 and 1550 cm^{-1}. The associated

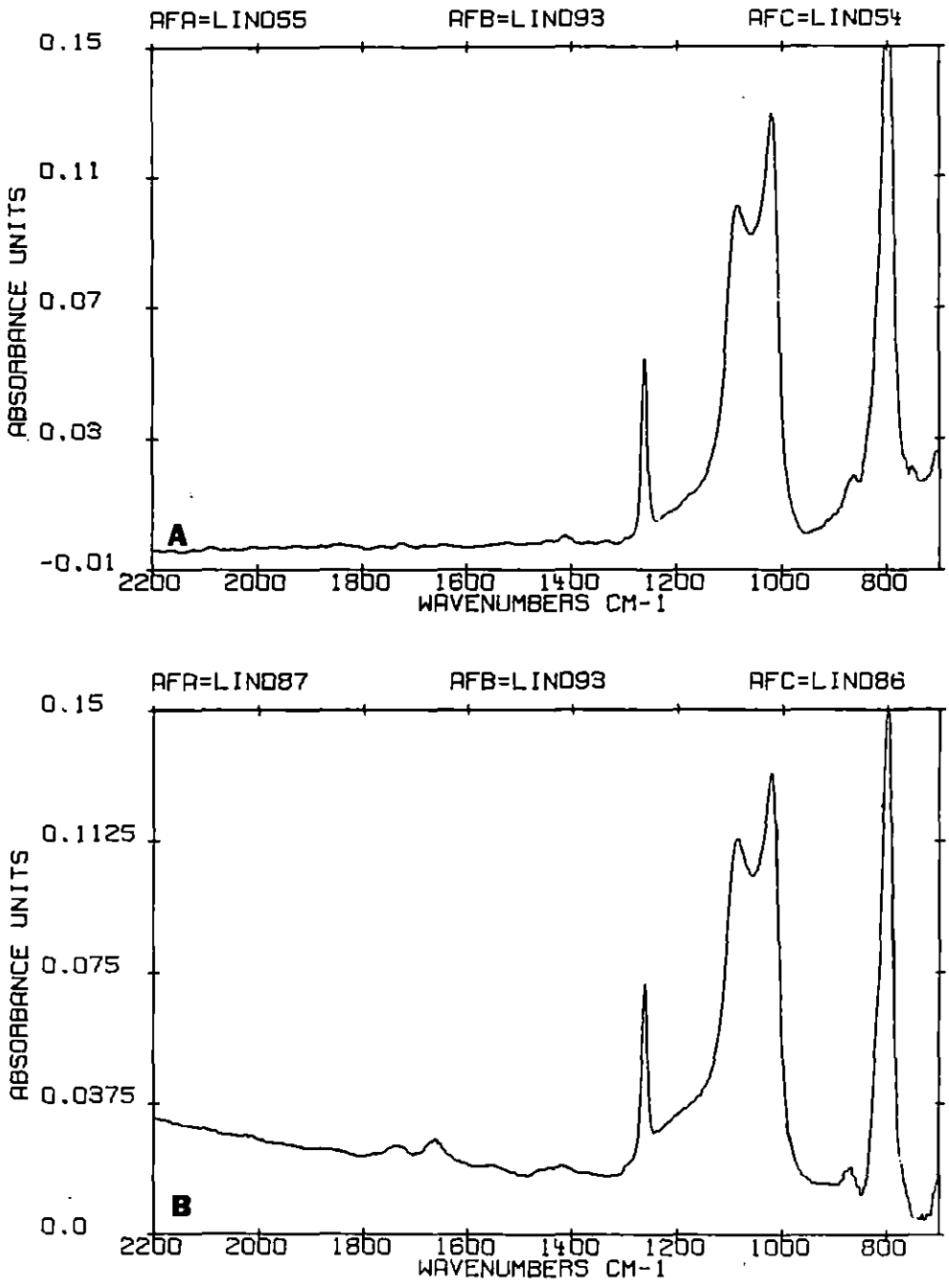

FIGURE 24. Absorbance spectra showing water retention of silicone rubber (A) and 5% HEMA/15% NVP (B)

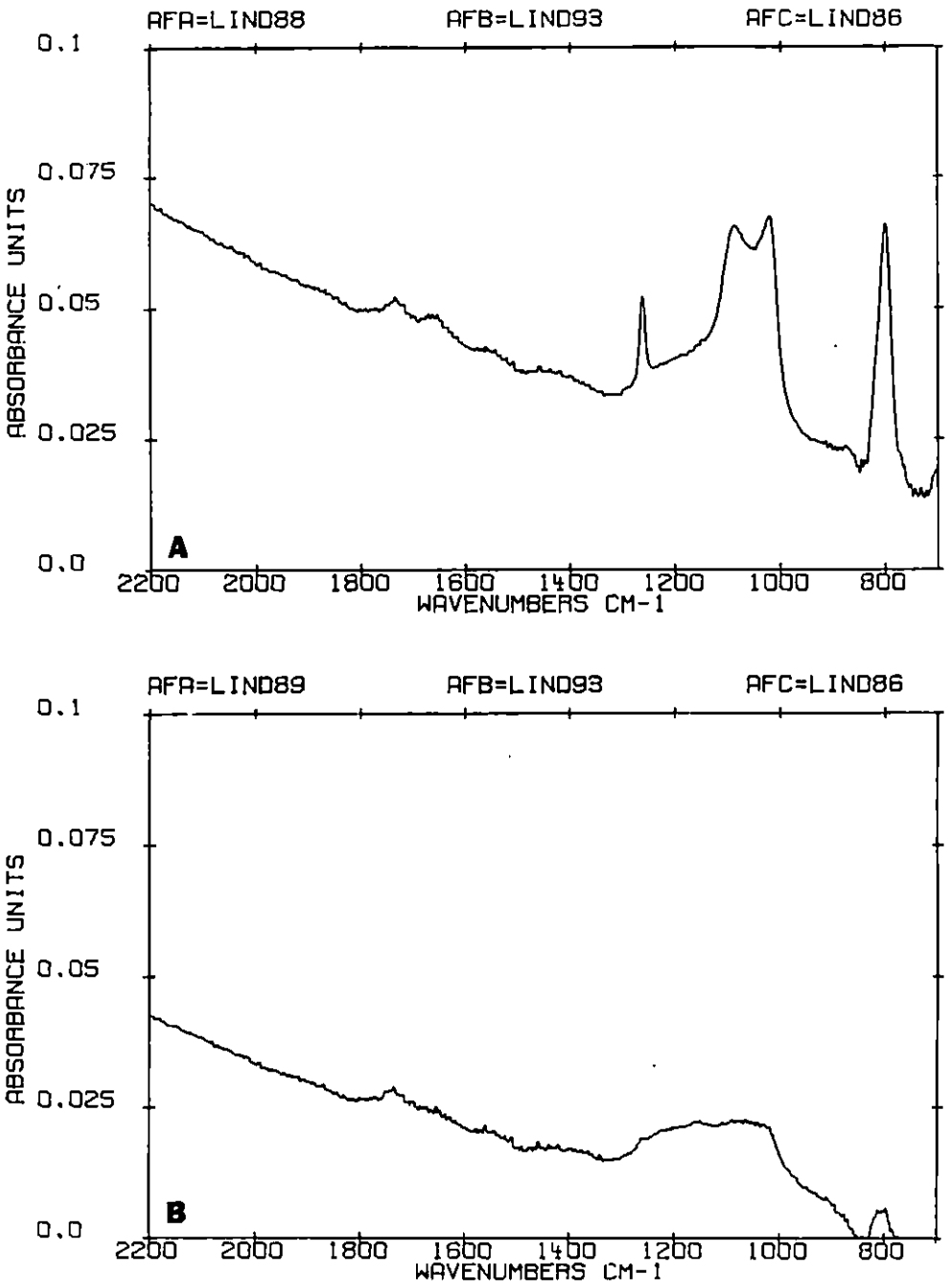

FIGURE 25. Absorbance spectra showing water retention of 10% HEMA/10% NVP (A) and 15% HEMA/5% NVP (B)

microstructural information for each FT-IR spectrum permits an insight into the nature of the organization and types of blood elements which have been deposited. Then, comparisons can be made among dogs to examine consistency for relative amounts of protein deposited and the nature of microstructural features observed. Comparisons can also be made with respect to time by comparing the initial implant series with the second implant series. In most cases, where fibrin and cellular deposition is heavy, the FT-IR spectra show relatively large protein peaks at 1650 and 1550 cm^{-1}. Likewise, where the surface appears clean, the corresponding IR spectra have minimal to no protein peaks. Apparent discrepancies may be explained by the fact that, although the SEM micrographs and the FT-IR spectra were obtained from the same piece of sample, the SEM micrographs were taken of one half, while the IR spectra were collected from the other half.

Figures 26a through 26t represent FT-IR spectra and the corresponding SEM micrographs from dog 3178. Within Figure 26, the 15% HEMA/5% NVP surfaces appear to have the least deposition of fibrin and formed elements based on the SEM micrographs (L and T). The associated IR spectra (D and H) indicate lower relative intensities of the protein bands compared with the other formulations. The silicone rubber and 5% HEMA/15% NVP surfaces were the most extensively

covered. Within all similar formulations, comparisons by SEM indicate relatively more fibrin, or a more open network of fibrin, and more red cells on the left leg samples than on the right leg samples (inserted first). Similarly, the IR spectra of the left leg samples had larger protein peaks for similar formulations. For example, A,I (left leg) compared with E, N (right leg) for silicone rubber; B, J (left leg) compared with F, O, P (right leg) for 5% HEMA/15% NVP, and so on. Relatively more protein was observed on the less hydrophilic hydrogels (i.e., 5% HEMA/15% NVP) than on the more hydrophilic hydrogels (15% HEMA/5% NVP and 10% HEMA/10% NVP), as seen in a comparison of FT-IR spectra for the three dogs and as summarized in Table 4. The cleanest surface (least adherent) was 15% HEMA/5% NVP at the common 15 minute exposure time and represents a time when the most deposition is seen for all formulations examined (Vale and Greer, ca. 1982). After 15 to 30 minutes, deposits on hydrophilic surfaces are relatively sparse and perhaps more readily sloughed off or desorbed compared with hydrophobic surfaces (e.g., silicone rubber).

Figures 27a through 27q represent FT-IR spectra and the associated SEM micrographs for the dog G.S. In Figure 27, almost all surfaces were clean, having only a few white cells and platelets. The exceptions were silicone rubber and 5% HEMA/15% NVP from the left leg.

Figures 28a through 28s represent FT-IR spectra and SEM micrographs from dog 3172. Again, the 15% HEMA/5% NVP surfaces from both legs showed the least adherent material, although a few other surfaces (5% HEMA/15% NVP and silicone rubber) were also clean. Comparisons of FT-IR spectra of the left (implanted second) and the right (implanted first) leg samples indicate slightly more protein on the left leg samples.

Trends were identical in each dog for each formulation and comparisons among formulations with respect to relative amounts of protein and relative microstructural features of deposits. Even though dog to dog variations were observed, 15% HEMA/5% NVP had the least deposition of fibrin at the 15 minute exposure.

FIGURE 26. (continued on pages 79, 80, and 81). FT-IR spectra and associated SEM micrographs for dog 3178. Sample pairs are designated: left leg (right leg)

Formulation	FT-IR	SEM
silicone rubber	A (E)	I (N)
5% HEMA/15% NVP	B (F)	J (O,P)
10% HEMA/10% NVP	C (G)	K (Q,R)
15% HEMA/5% NVP	D (H)	L,M (S,T)

(scale bar=10 μm)

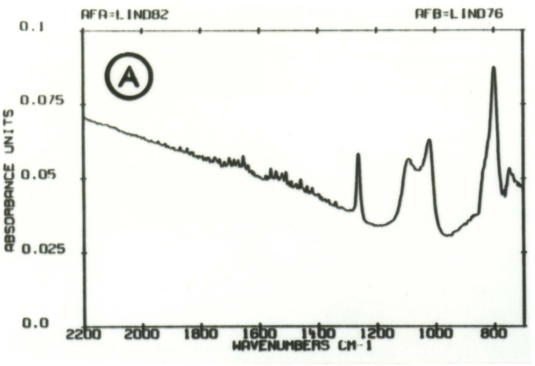
AFA=LIND82
AFB=LIND76
A
0.1
0.075
0.05
0.025
0.0
ABSORBANCE UNITS
2200 2000 1800 1600 1400 1200 1000 800
WAVENUMBERS CM-1

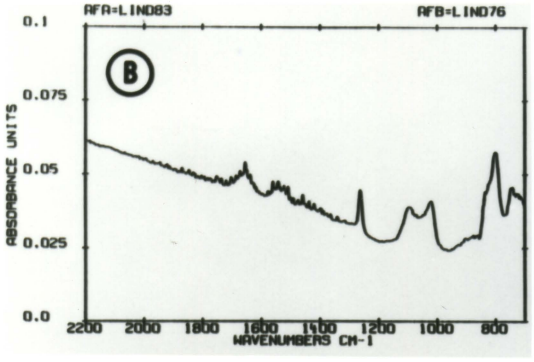
AFA=LIND83
AFB=LIND76
B
0.1
0.075
0.05
0.025
0.0
ABSORBANCE UNITS
2200 2000 1800 1600 1400 1200 1000 800
WAVENUMBERS CM-1

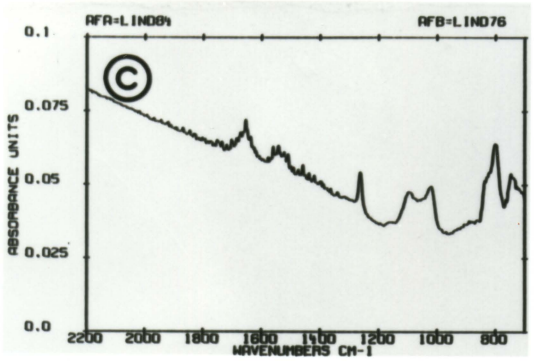
AFA=LIND84
AFB=LIND76
C
0.1
0.075
0.05
0.025
0.0
ABSORBANCE UNITS
2200 2000 1800 1600 1400 1200 1000 800
WAVENUMBERS CM-1

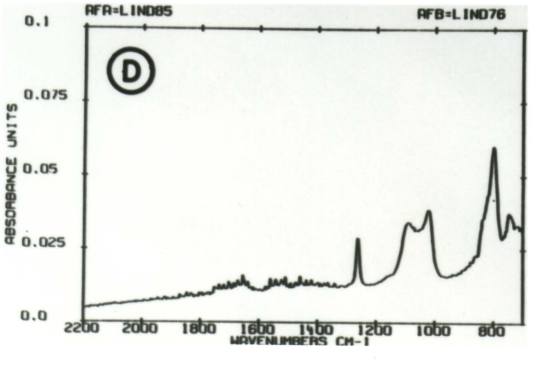
AFA=LIND85
AFB=LIND76
D
0.1
0.075
0.05
0.025
0.0
ABSORBANCE UNITS
2200 2000 1800 1600 1400 1200 1000 800
WAVENUMBERS CM-1

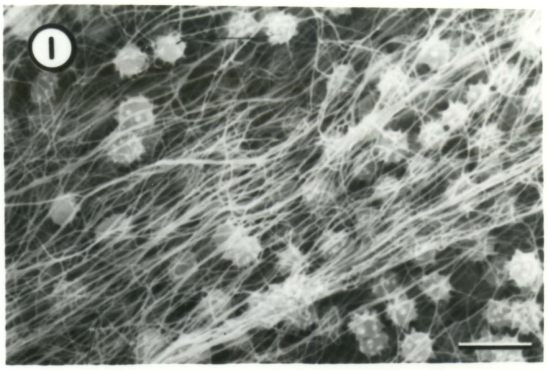
I

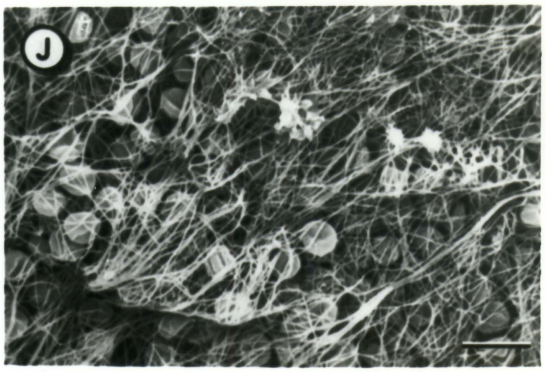
J

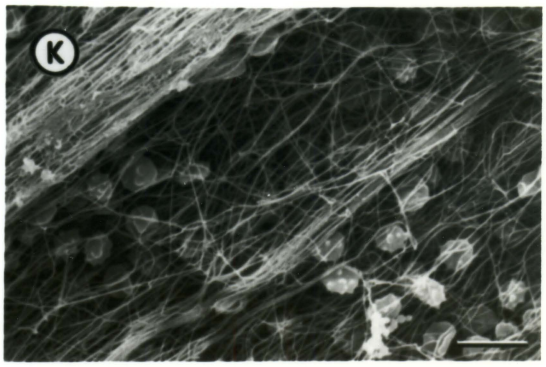
K


L

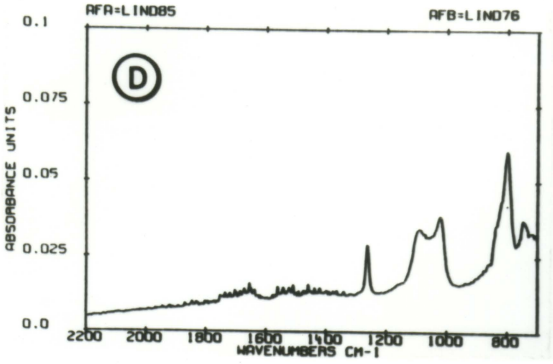
AFA=LIND85
AFB=LIND76
D
ABSORBANCE UNITS
0.1
0.075
0.05
0.025
0.0
2200 2000 1800 1600 1400 1200 1000 800
WAVENUMBERS CM-1

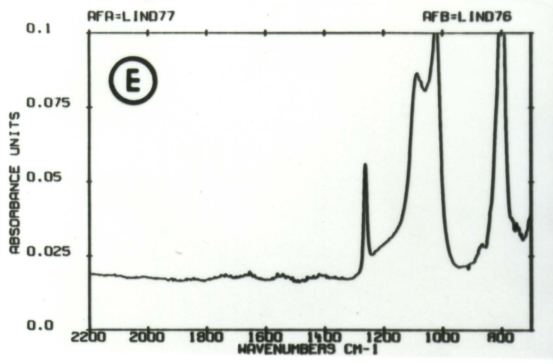
AFA=LIND77
AFB=LIND76
E
ABSORBANCE UNITS
0.1
0.075
0.05
0.025
0.0
2200 2000 1800 1600 1400 1200 1000 800
WAVENUMBERS CM-1

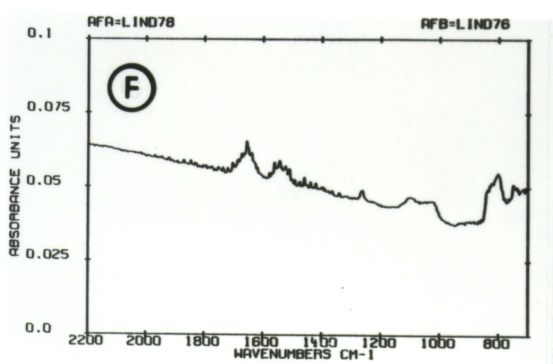
AFA=LIND78
AFB=LIND76
F
ABSORBANCE UNITS
0.1
0.075
0.05
0.025
0.0
2200 2000 1800 1600 1400 1200 1000 800
WAVENUMBERS CM-1

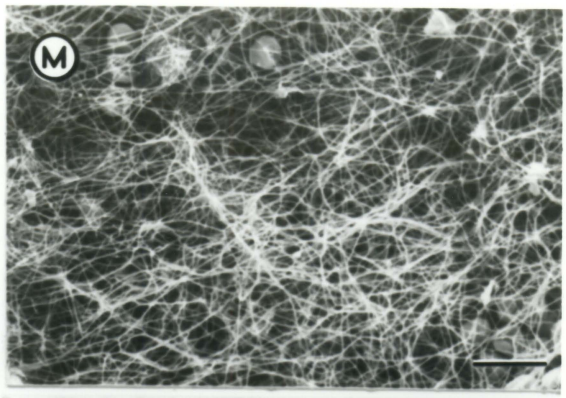
M

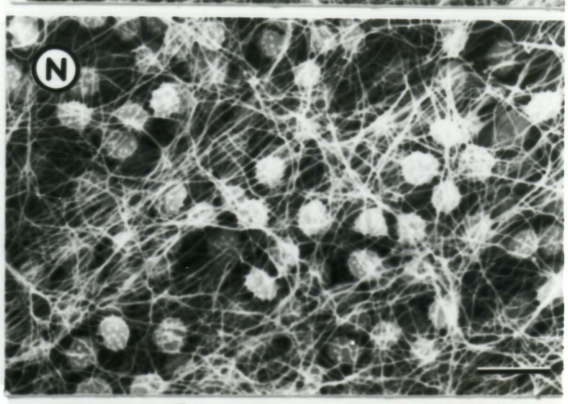
N

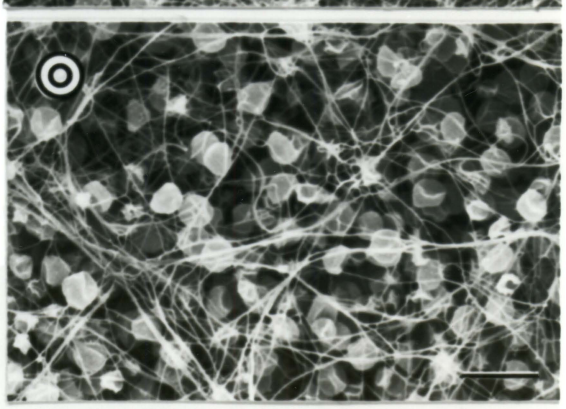
O


P

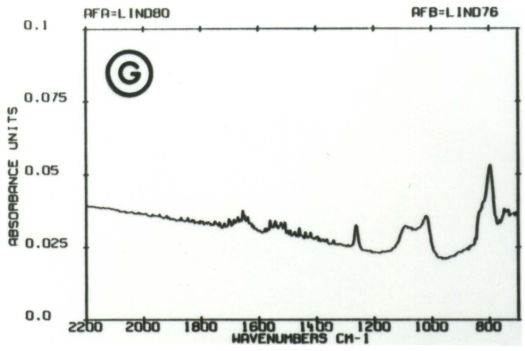
AFA=LIND80
AFB=LIND76
G
0.1
0.075
0.05
0.025
0.0
ABSORBANCE UNITS
2200 2000 1800 1600 1400 1200 1000 800
WAVENUMBERS CM-1

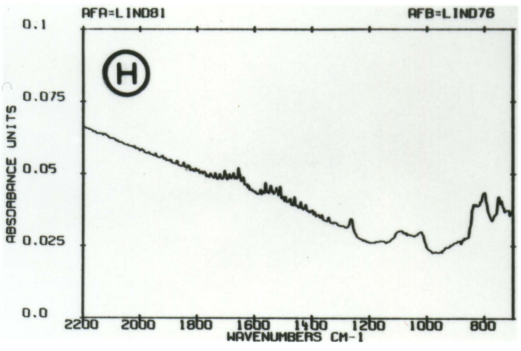
AFA=LIND81
AFB=LIND76
H
0.1
0.075
0.05
0.025
0.0
ABSORBANCE UNITS
2200 2000 1800 1600 1400 1200 1000 800
WAVENUMBERS CM-1


Q

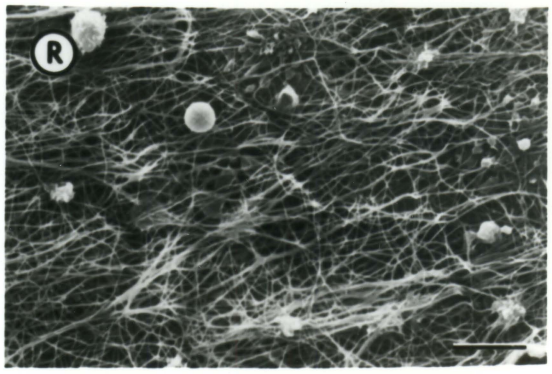
R

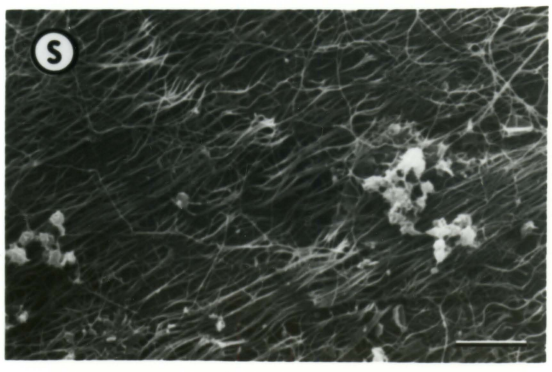
S

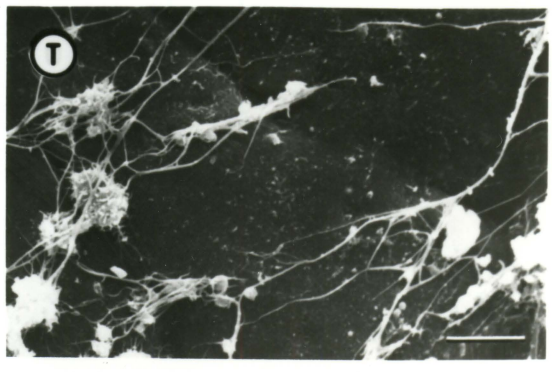
T

FIGURE 27. (continued on pages 83, 84, and 85). FT-IR spectra and associated SEM micrographs for dog G.S. Sample pairs are designated: left leg (right leg)

Formulation	FT-IR	SEM
silicone rubber	A (E)	I (N)
5% HEMA/15% NVP	B (F)	J,K (O)
10% HEMA/10% NVP	C (G)	L (P)
15% HEMA/5% NVP	D (H)	M (Q)

(scale bar=10 μm)

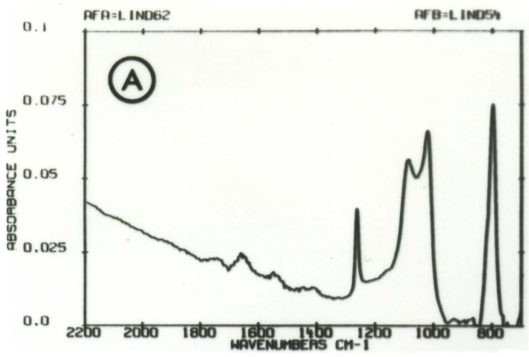
AFA=LIND62
AFB=LIND5%
A
0.1
0.075
0.05
0.025
0.0
ABSORBANCE UNITS
2200 2000 1800 1600 1400 1200 1000 800
WAVENUMBERS CM-1

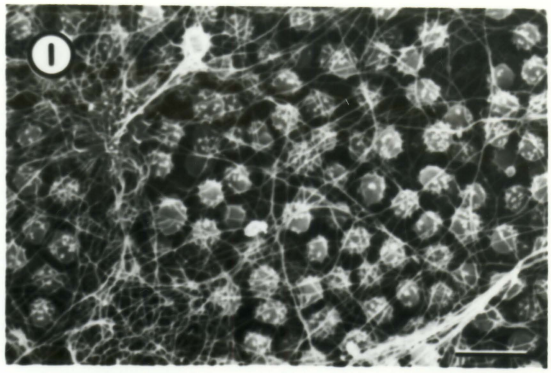
I

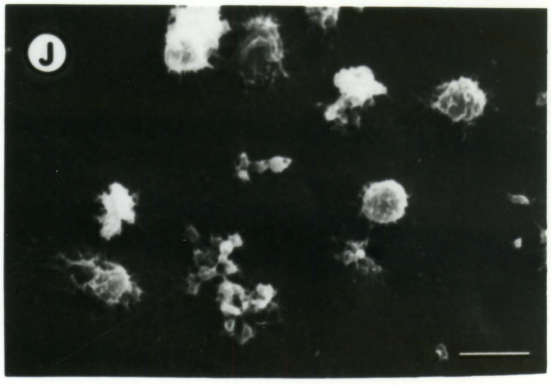
J

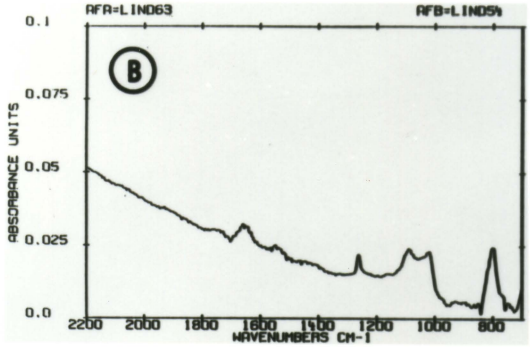
AFA=LIND63
AFB=LIND5%
B
0.1
0.075
0.05
0.025
0.0
ABSORBANCE UNITS
2200 2000 1800 1600 1400 1200 1000 800
WAVENUMBERS CM-1

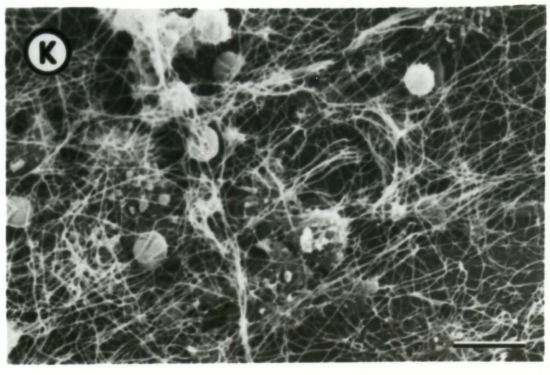
K

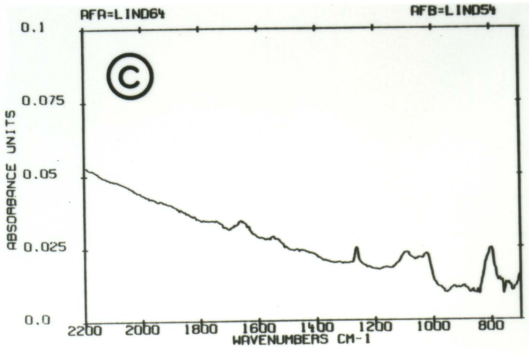
AFA=LIND64
AFB=LIND5%
C
0.1
0.075
0.05
0.025
0.0
ABSORBANCE UNITS
2200 2000 1800 1600 1400 1200 1000 800
WAVENUMBERS CM-1

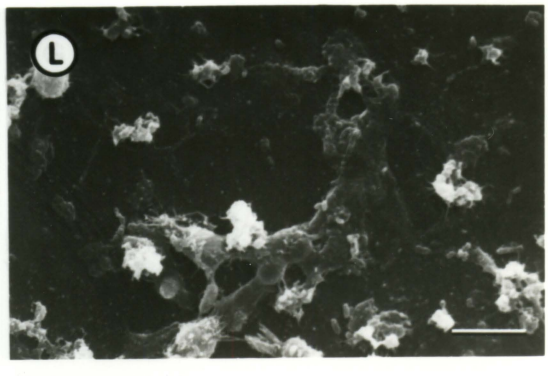
L

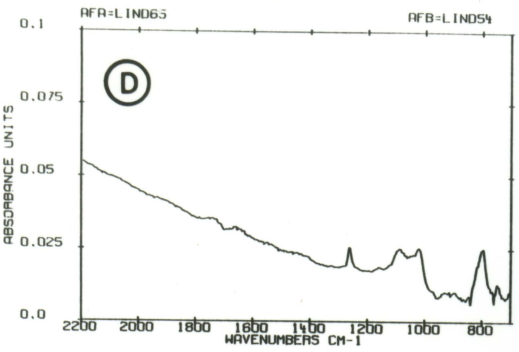
AFA=LIND65
AFB=LIND54
D
ABSORBANCE UNITS
0.1
0.075
0.05
0.025
0.0
2200 2000 1800 1600 1400 1200 1000 800
WAVENUMBERS CM-1

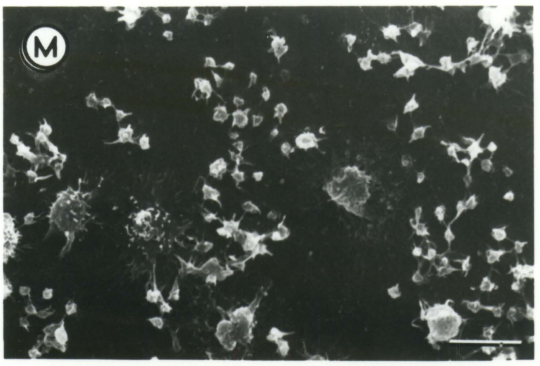
M

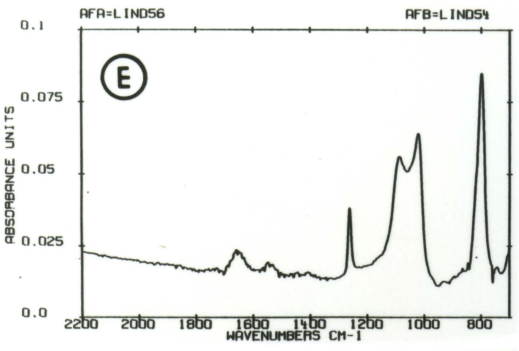
AFA=LIND56
AFB=LIND54
E
ABSORBANCE UNITS
0.1
0.075
0.05
0.025
0.0
2200 2000 1800 1600 1400 1200 1000 800
WAVENUMBERS CM-1

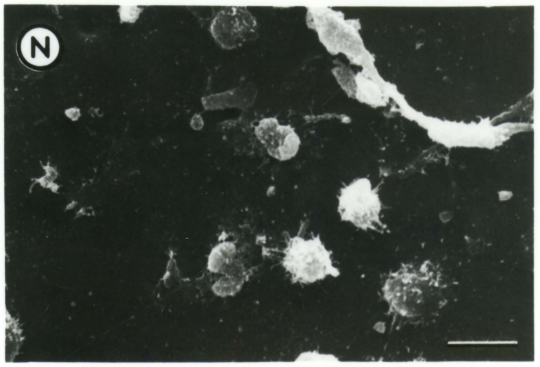
N

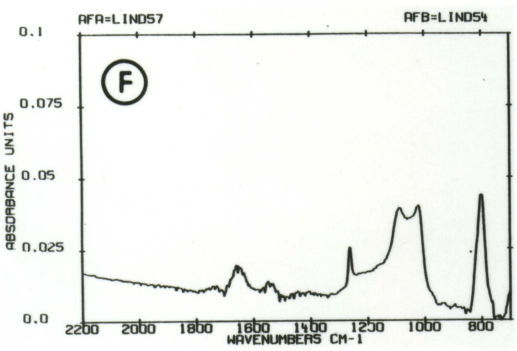
AFA=LIND57
AFB=LIND54
F
ABSORBANCE UNITS
0.1
0.075
0.05
0.025
0.0
2200 2000 1800 1600 1400 1200 1000 800
WAVENUMBERS CM-1

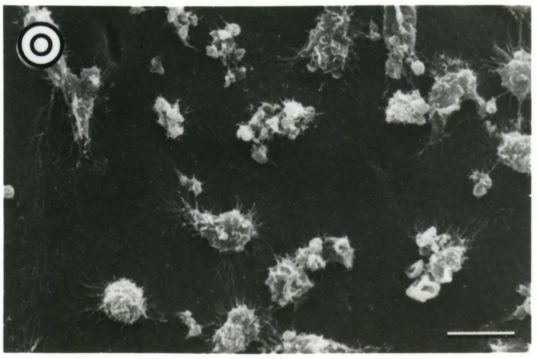
O

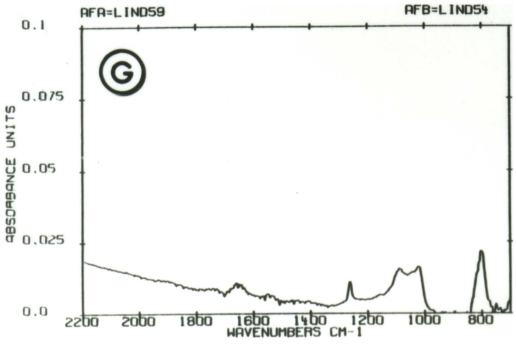
AFA=LIND59
AFB=LIND54
G
ABSORBANCE UNITS
0.1
0.075
0.05
0.025
0.0
2200 2000 1800 1600 1400 1200 1000 800
WAVENUMBERS CM-1

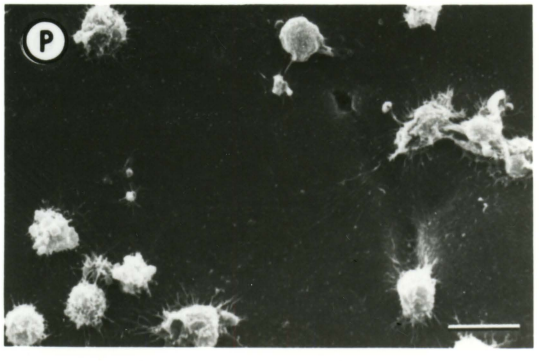
P

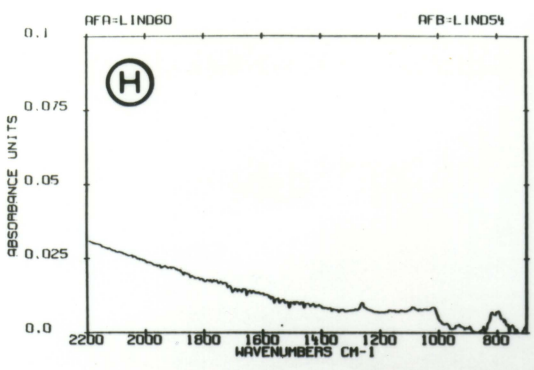
AFA=LIND60
AFB=LIND54
H
0.1
0.075
0.05
0.025
0.0
ABSORBANCE UNITS
2200
2000
1800
1600
1400
1200
1000
800
WAVENUMBERS CM-1

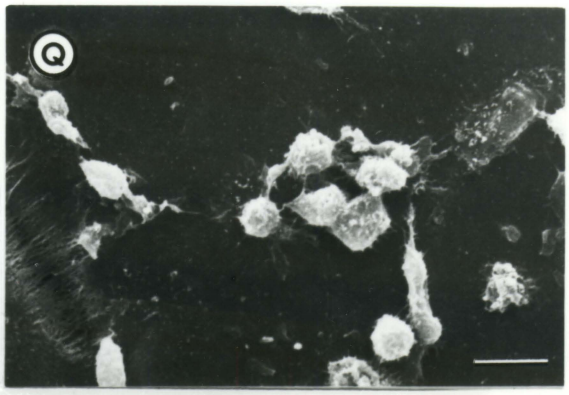
Q

FIGURE 28. (continued on pages 87, 88, and 89). FT-IR spectra and associated SEM micrographs for dog 3172. Sample pairs are designated: left leg (right leg)

Formulation	FT-IR	SEM
silicone rubber	A (E)	I (N,O)
5% HEMA/15% NVP	B (F)	J (K,P)
10% HEMA/10% NVP	C (G)	L (Q,R)
15% HEMA/5% NVP	D (H)	M (S)

(scale bar I=3.3 μm, scale bar J-S=10 μm)

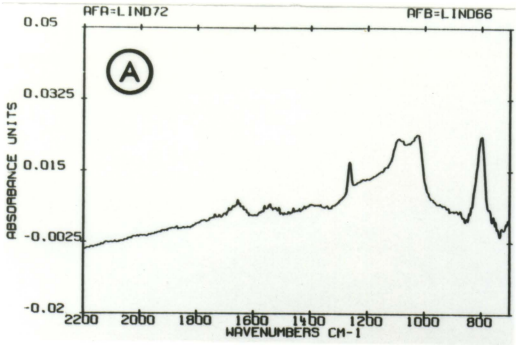
AFA=LIND72
AFB=LIND66
A
0.05
0.0325
0.015
-0.0025
-0.02
ABSORBANCE UNITS
2200 2000 1800 1600 1400 1200 1000 800
WAVENUMBERS CM-1

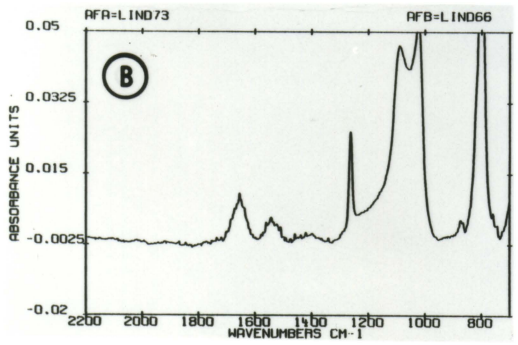
AFA=LIND73
AFB=LIND66
B
0.05
0.0325
0.015
-0.0025
-0.02
ABSORBANCE UNITS
2200 2000 1800 1600 1400 1200 1000 800
WAVENUMBERS CM-1

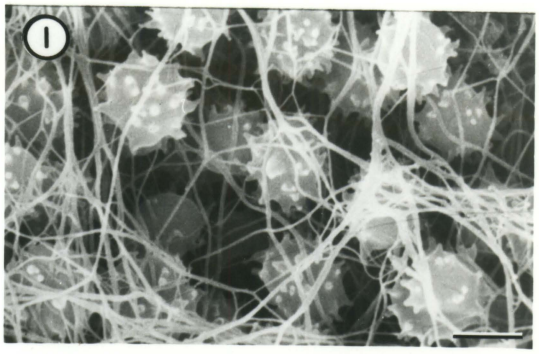
I

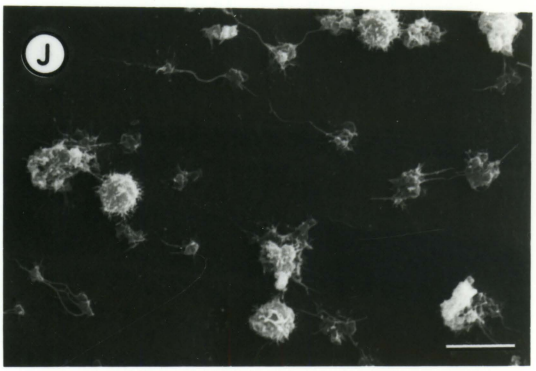
J

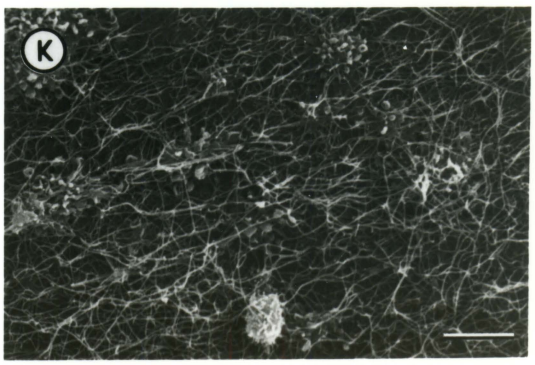
K

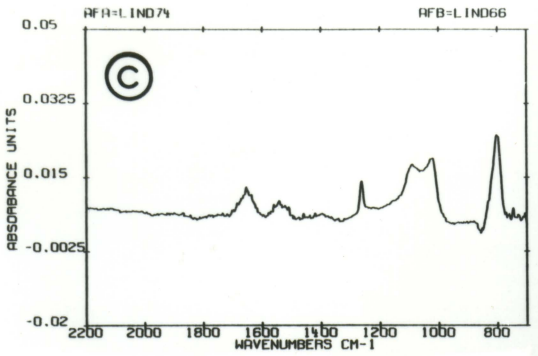
AFA=LIND74
AFB=LIND66
C
0.05
0.0325
0.015
-0.0025
-0.02
ABSORBANCE UNITS
2200 2000 1800 1600 1400 1200 1000 800
WAVENUMBERS CM-1

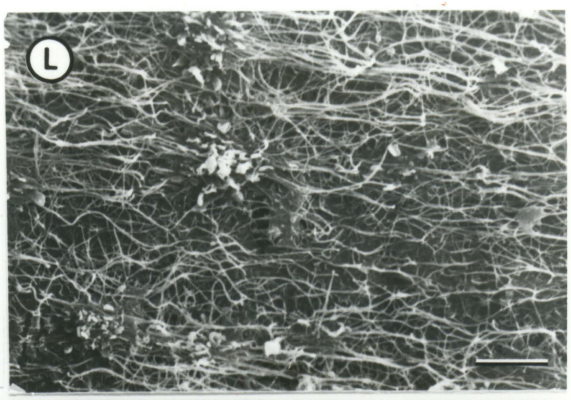
L

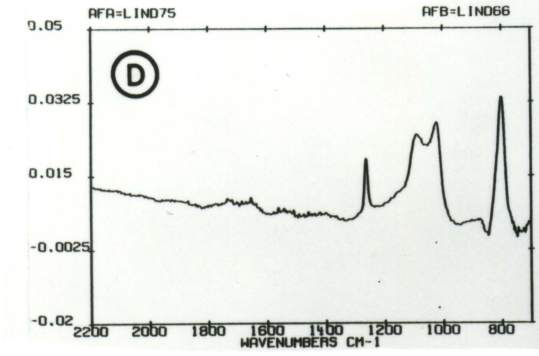
AFA=LIND75
AFB=LIND66
D
0.05
0.0325
0.015
-0.0025
-0.02
2200 2000 1800 1600 1400 1200 1000 800
WAVENUMBERS CM-1


M

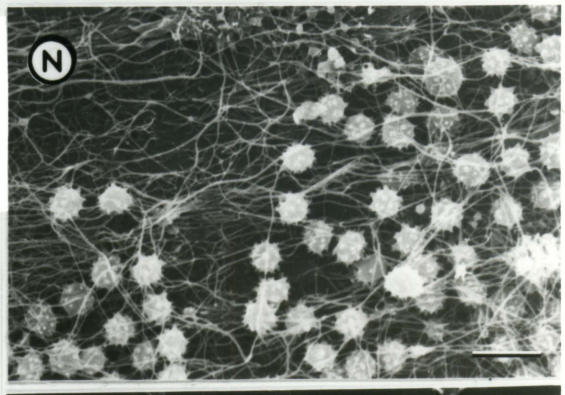
N

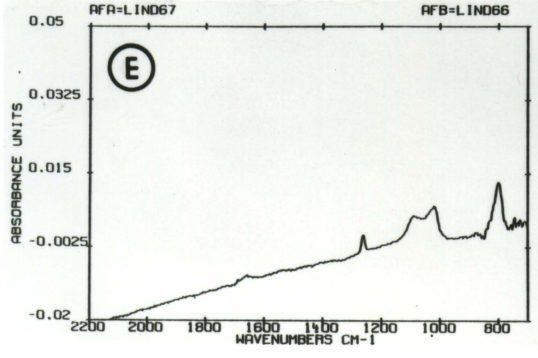
AFA=LIND67
AFB=LIND66
E
0.05
0.0325
0.015
-0.0025
-0.02
ABSORBANCE UNITS
2200 2000 1800 1600 1400 1200 1000 800
WAVENUMBERS CM-1

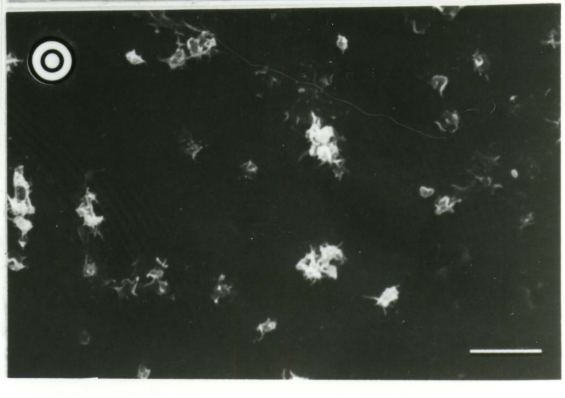
O

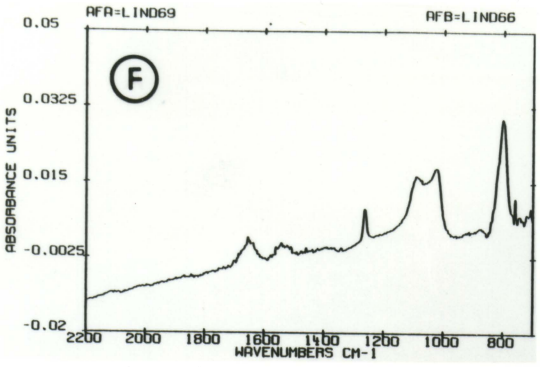
AFA=LIND69
AFB=LIND66
F
0.05
0.0325
0.015
-0.0025
-0.02
ABSORBANCE UNITS
2200 2000 1800 1600 1400 1200 1000 800
WAVENUMBERS CM-1

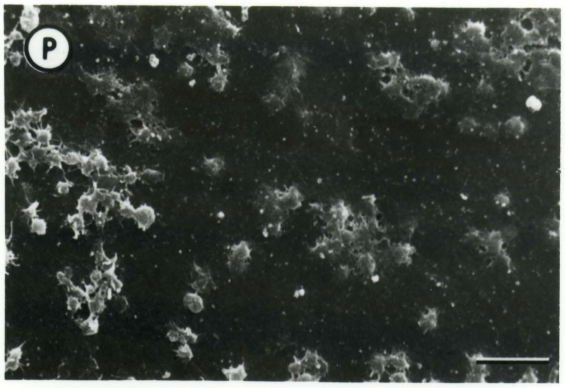
P

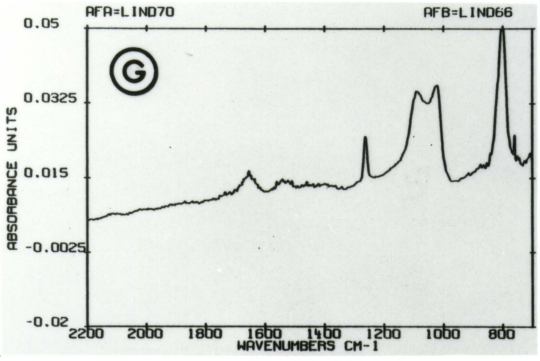
AFA=LIND70
AFB=LIND66
G
0.05
0.0325
0.015
-0.0025
-0.02
ABSORBANCE UNITS
2200 2000 1800 1600 1400 1200 1000 800
WAVENUMBERS CM-1

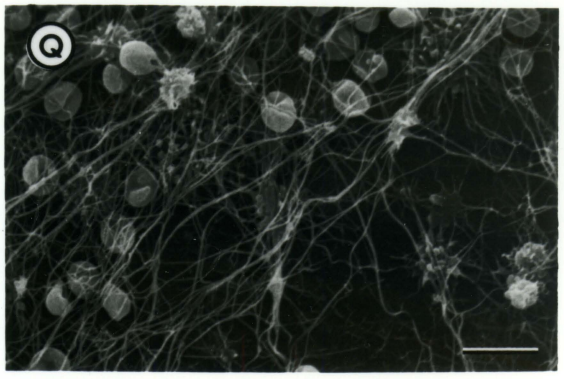
Q

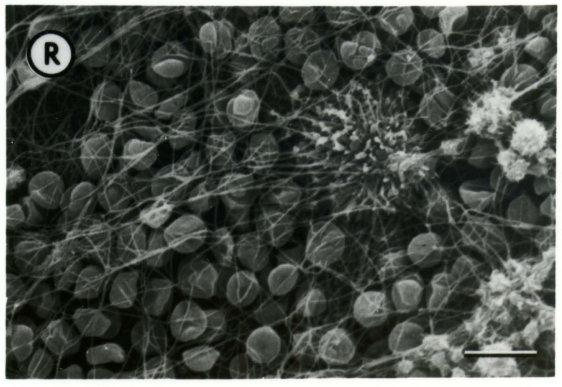
R

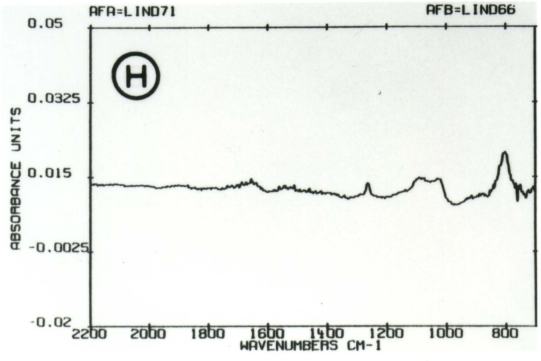
AFA=LIND71
AFB=LIND66
H
0.05
0.0325
0.015
-0.0025
-0.02
ABSORBANCE UNITS
2200 2000 1800 1600 1400 1200 1000 800
WAVENUMBERS CM-1

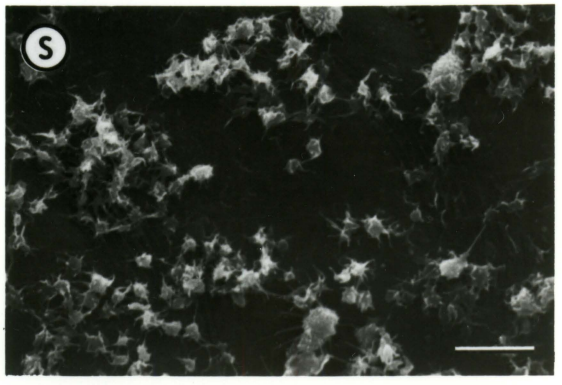
S

CONCLUSION

This work represents the first attempt to relate FT-IR, used to monitor protein deposition, with microstructural features revealed by SEM. The materials tested were silicone rubber, 5% HEMA/15% NVP, 10% HEMA/10% NVP, and 15% HEMA/5% NVP. It was possible to demonstrate major, reproducible differences in the response of blood to the different surfaces using combined SEM and FT-IR. The responses to the four materials, compared within and among dogs, were consistent. In general, the more hydrophilic hydrogel grafted surfaces showed less deposition of fibrin and cellular elements than the ungrafted hydrophobic silicone rubber samples. In particular, the 15% HEMA/5% NVP surface was the least adherent of the hydrogel formulations investigated. The largest quantities of fibrin and entrapped red cells were noted on the silicone rubber samples. It is believed that the hydrophilic nature of the 15% HEMA/5% NVP surface resulted in relatively decreased adhesion of blood elements, and the hydrophobic nature of the silicone rubber samples resulted in relatively increased adhesion. As a general observation, the relative intensities of the protein peaks on the IR spectra correspond to the different amounts of protein deposited among the four materials. The quantity of material, represented by microstructural features observed using SEM,

tended to parallel the relative intensities of the protein peaks. Relatively large protein peaks on the IR spectra, indicating relatively large quantities of protein, corresponded to extensive networks of fibrin and formed elements on the associated SEM micrographs.

Comparison of samples which were implanted in the left leg (second), and those implanted in the right leg (first), usually revealed larger protein peaks by FT-IR and more fibrin and formed elements by SEM on the second set of samples. It is believed that exposure of the first set of samples to blood stimulated the immune response, causing a more severe reaction to the second set of samples.

Observations by FT-IR of the hydrogel grafted silicone rubber samples, compared to the ungrafted silicone rubber, indicate increasing graft with increasing percent HEMA, expressed as a HEMA/NVP ratio, as evidenced by the decreasing intensity of the silicone rubber peaks.

Individual proteins were not distinguished by FT-IR of the samples which were exposed to blood. A possible explanation for this arises from the inability to do perfect subtractions of the spectra of the underlying polymer from the spectra of the polymers with adsorbed proteins. In this investigation, the spectra of the four materials were collected at one time, while the spectra of the protein coated materials were collected at a different time.

Variations in samples size, position, and relative pressure on the ATR crystal, as well as alignment of the ATR crystal in the beam path, are all sources of problems. To achieve a perfect subtraction, it would be necessary to collect a spectrum of the polymer, expose the polymer to blood, and collect another spectrum, without moving the crystal or the polymer. This could be accomplished by coating the ATR crystal with the polymer of interest, flowing blood past the coated crystal, collecting the appropriate spectra, and then subtracting the spectrum of the polymer from the spectrum of the protein coated polymer. This subtraction is much more accurate because the experimental arrangement allows the beam to completely penetrate the polymer thus eliminating the need to scale the spectrum of the polymer before subtraction.

BIBLIOGRAPHY

Andrade, J D. 1973. Interfacial phenomena and biomaterials. Medical Instrumentation 7(2):110-120.

Andrade, J. D., H. B. Lee, M. S. Jhon, S. W. Kim, and J. B. Hibbs, Jr. 1973. Water as a biomaterial. Trans. Am. Soc. Artif. Intern. Organs 19:1-7.

Bagnall, R. D. 1977. Adsorption of plasma proteins on hydrophobic surfaces. I. Albumin and gamma globulin. J. Biomed. Mater. Res. 11:947-978.

Baier, R. E. 1977. The organization of blood components near interfaces. Annals New York Academy of Sciences 283:17-36.

Baier, R. E. and R. E. Dutton. 1969. Initial events in interactions of blood with a foreign surface. J. Biomed. Mater. Res. 3:191-206.

Barber, T. A., L. K. Lambrecht, D. L. Mosher, and S. L. Cooper. 1979. Influence of serum proteins on thrombosis and leucocyte adherence on polymer surfaces. Scanning Electron Microscopy 3:881-890.

Barber, T. A., T. Mathis, J. V. Ihlenfeld, S. L. Cooper, and D. F. Mosher. 1978. Short term interactions of blood with polymeric vascular graft materials: Protein adsorption, thrombus formation, and leucocyte deposition. Scanning Electron Microscopy 2:431-440.

Brash, J. L. and D. J. Lyman. 1969. Adsorption of plasma proteins in solution to uncharged hydrophobic polymer surfaces. J. Biomed Mater. Res. 3:175-189.

Brash, J. L. and S. Uniyal. 1979. Dependence of albumin and fibrinogen simple and competitive adsorption on surface properties of biomaterials. J. Polymer Science: Polymer Symposium 66, 377-389.

Brash, J. L. and S. Uniyal. 1976. Adsorption of albumin and fibrinogen to polyethylene in presence of red cells. Trans. Am. Soc. Artif. Intern. Organs 22:253-259.

Conley, R. T. 1972. Infrared spectroscopy. Allyn and Bacon, Inc., Boston.

Dillman, Jr., W. J. and I. F. Miller. 1973. On the adsorption of serum proteins on polymer membrane surfaces. J. Colloid Interface Sci. 44(2):221.

Garcia, C., J. M. Anderson, and S. A. Barenberg. 1980. Hemocompatibility: Effect of structured water. Trans. Am. Soc. Artif. Intern. Organs 26:294-298.

Gendreau, R. M. and R. J. Jakobsen. 1979. Blood surface interactions: Fourier Transform infrared studies of protein surface adsorption from flowing whole blood and serum. J. Biomed. Mater. Res. 13:893-906.

Gendreau, R. M., R. I. Leininger, L. L. Brown, S. Winters, and R. J. Jakobsen. ca. 1982a. An FT-IR comparison of whole blood-polymer interactions. J. Amer. Soc. Art. Intern. Organs in press.

Gendreau, R. M., R. I. Leininger, S. Winters, and R. J. Jakobsen. ca. 1982b. Chapter in S. Cooper, A. Hoffman, B. Ratner, and N. Peppas, eds. The morphology, structure, and interactions of biomaterials. A. C. S. Adv. Chem. Ser., Washington, D. C.

Gendreau, R. M., S. Winters, R. I. Leininger, D. Fink, C. R. Hassler, and R. J. Jakobsen. 1981. Fourier Transform infrared spectroscopy of protein adsorption from whole blood: Ex vivo dog studies. Applied Spectroscopy 35(4):353-357.

Hoffman, A. S., T. A. Horbett, and B. D. Ratner. 1977. Interactions of blood and blood components at hydrogel interfaces. Annals New York Academy of Sciences 283:372-382.

Holly, F. J. 1979. Protein and lipid adsorption by acrylic hydrogels and their relation to water wettability. J. Polymer Science: Polymer Symposium 66, 409-417.

Holly, F. J. and M. F. Refojo. 1976. Water wettability of hydrogels. Pages 252-266 in J. D. Andrade, ed. Hydrogels for medical and related applications. American Chemical Society, Washington, D. C.

Holly, F. J. and M. F. Refojo. 1975. Wettability of hydrogels. I. Poly(2-hydroxyethyl methacrylate). J. Biomed. Mater. Res. 9:315-326.

Horbett, T. A. and A. S. Hoffman. 1975. Bovine plasma protein adsorption onto radiation grafted hydrogels based on hydroxyethyl methacrylate and N-vinylpyrrolidone. Pages 230-254 in R. F. Gould, ed. Applied chemistry at protein interfaces. A.C.S. Adv. Chem. Ser, Washington, D. C.

Ihlenfeld, J. V. and S. L. Cooper. 1979. Transient in vivo protein adsorption to polymeric biomaterials. J. Biomed. Mater. Res. 13:577-591.

Jakobsen, R. J. and R. M. Gendreau. 1978. FT-IR studies of adsorption on polyethylene and heparin treated polyethylene surfaces. Artificial Organs 2(2):183-188.

Jakobsen, R. J., L. L. Brown, S. Winters, and R. M. Gendreau. ca. 1982a. Effects of flow rate and solution concentration on in situ protein adsorption behavior. J. Biomed. Mater. Res. in press.

Jakobsen, R. J., R. M. Gendreau, S. Winters, L. L. Brown, and R. I. Leininger. ca. 1982b. Chapter in K. Mittal, ed. Physical, chemical aspects of polymer surfaces. VIII. Biomedical aspects and bioadhesion. Plenum Press in press.

Jakobsen, R. J., S. Winters, and R. M. Gendreau. 1981. Biological applications of FT-IR and bloody FT-IR. Page 469 in H. Sakai, ed. Proceedings of the international conference on Fourier Transform Infrared Spectroscopy, vol. 289. S.P.I.E.-The International Society for Optical Engineering, held at Columbia, S. Carolina.

Jhon, M. S. and J. D. Andrade. 1973. Water and hydrogels. J. Biomed. Mater. Res. 7:509-522.

Kim, S. W. and R. G. Lee. 1975. Adsorption of blood proteins onto polymer surfaces. Adv. Chem. Ser. 145:218-229.

Kim, S. W., S. Wisniewski, E. S. Lee, and M. L. Winn. 1977. Role of protein and fatty acid adsorption on platelet adhesion and aggregation at the blood-polymer interface. J. Biomed. Mater. Res. Symp. 8:23-31.

Kim, S. W., R. G. Lee, H. Oster, D. Coleman, J. D. Andrade, D. J. Lentz, D. Olsen. 1974. Platelet adhesion to polymer surfaces. Trans. Am. Soc. Artif. Intern. Organs 20:449-455.

Koenig, J. L. and D. L. Tabb. 1980. Infrared spectra of globular proteins in aqueous solution. NATO Adv. Study Inst. Series C. Math and Physical Sciences, vol. 57. Anal. Applications of FT-IR to molecular and biological systems. Proceedings of the NATO Adv. Study Inst. held at Florence, Italy. J. R. Durig, ed. D. Reidel Pub. Co., Boston.

Lee, R. G. and S. W. Kim. 1974. The role of carbohydrate in platelet adhesion to foreign surfaces. J. Biomed. Mater. Res. 8:393-398.

Lee, R. G., C. Adamson, and S. W. Kim. 1974. Competitive adsorption of plasma proteins onto polymer surfaces. Thrombosis Research 4:485-490.

Lyman, D. J., L. C. Metcalf, D. Albo, Jr., K. F. Richards, and J. Lamb. 1974. The effect of chemical structure and surface properties of synthetic polymers on the coagulation of blood. III. In vivo adsorption of proteins on polymer surfaces. Trans. Am. Soc. Artif. Intern. Organs 20:474-478.

Lyman, D. J., J. L. Brash, and K. G. Klein. 1969. The effect of chemical structure and surface properties of synthetic polymers on the coagulation of blood. Pages 113-121 in R. J. Hegyeli, M. D., ed. Proceedings Artificial Heart Program Conference. U. S. Government Printing Office, Washington, D. C.

Lyman, D. J., J. L. Brash, S. W. Chaikin, and K. G. Klein, M. Carini. 1968. The effect of chemical structure and surface properties of synthetic polymers on the coagulation of blood. II. Protein and platelet interaction with polymer surfaces. Trans. Am. Soc. Artif. Intern. Organs 14:250-255.

Mason, R. G., M. S. Read, and K. M. Brinkhaus. 1971. Effect of fibrinogen concentration on platelet adhesion to glass. P. S. E. B. M. 137:680-682.

Nakashima, T., K. Takakura, and Y. Komoto. 1977. Thromboresistance of graft-type copolymers with hydrophilic-hydrophobic microphase separated structure. J. Biomed. Mater. Res. 11:787-798.

Packham, M. A., G. Evans, M. F. Glynn, and J. F. Mustard. 1969. The effect of plasma proteins on the interactions of platelets with glass surfaces. J. Lab. Clin. Med. 73(4):686-697.

Ratner, B. D. and A. S. Hoffman. 1975. Radiation grafted polymers on silicone rubber as new biomaterials. Pages 159-171 in H. P. Gregor, ed. Biomedical applications of polymers. Plenum Pub. Corp., New York.

Roohk, H. V., M. Nakamura, R. L. Hill, E. K. Hung, and R. H. Bartlett. 1977. A thrombogenic index for blood contact materials. Trans. Am. Soc. Artif. Intern. Organs 23:152-161.

Roohk, H. V., J. Pick, R. Hill, E. Hung, and R. H. Bartlett. 1976. Kinetics of fibrinogen and platelet adherence to biomaterials. Trans. Am. Soc. Artif. Intern. Organs 22:1-7.

Vale, B. H. 1980. Hydrogel/silicone rubber composite materials: Fabrication, compatibility, and ex vivo blood responses. Ph.D. dissertation. Iowa State University, Ames, Iowa.

Vale, B. H. and R. T. Greer. ca. 1982. Ex vivo shunt testing of hydrogel/silicone rubber composite materials. J. Biomed. Mater. Res. in press.

Vroman, L., A. L. Adams, M. Klings, G. Fischer, and P. C. Munoz, R. P. Solensky. 1977. Reaction of formed elements of blood with plasma proteins at interfaces. Annals New York Academy of Sciences 283:65-76.

Watkins, R. W. and C. R. Robertson. 1977. A total internal-reflection technique for the examination of protein adsorption. J. Biomed. Mater. Res. 11:915-938.

Weathersby, P. K., T. A. Horbett, and A. S. Hoffman. 1977. Fibrinogen adsorption to surfaces of varying hydrophilicity. J. Bioeng. 1:395-410.

Weathersby, P. K., T. A. Horbett and A. S. Hoffman. 1976. A new method for analysis of the adsorbed plasma protein layer on biomaterial surfaces. Trans. Am. Soc. Artif. Organs 22:242-250.

Wichterle, O. and D. Lim. 1960. Hydrophilic gels in biological use. Nature (London) 185:117-118.

APPENDIX A

The following parameter set was used to collect, store, and plot the IR spectra.

AFA=LIND00	AFB=LIND00	AFC=LIND00	AFN=AS	APF=TR
APT=3	ASE=NO	BMS=6	BPA=0.0	BPC=1.0
BPD=1.0	CON=1.0	CSU=IN	DLY=200	DTC=MI
FLP=PHASE	FLR=LIND00	FLS=LIND00	GSG=1	HFQ=4500
HPF=6	LAB=LN	LFQ=0.0	LPF=0	LWN=15800
NFL=NEWFILE	NLV=0.000625	NSR=0	NSS=300	OFL=OLDFILE
OPF=3	PIP=64	PLF=TR	POP=SC	PTS=1024
RCH=BK	RES=4	RGN=-1	SCA=1.0	SCB=1.0
SCC=1.0	SCH=BK	SGN=-1	SMF=0	SPZ=NO
SRC=MI	XSL=200	XSP=2200	YMN=0.0	YMX=1.0
YSL=5.0	YCT=5	ZFF=4	XAX=YS	

APPENDIX B

Real time subtract commands (from IBM FT-IR instruction manual).

SAM - subtract absorbance manual - displays the two absorbance files AFA and AFB; plus the difference spectrum.

SSM - subtract spectrum manual - displays the two absorbance files created from single beam spectra in AFA, AFB, and, AFC, where AFC is the reference for both AFA and AFB; plus the difference spectrum.

STM - subtract transmittance manual - displays the two absorbance files created from the two transmittance files AFA and AFB; plus the difference spectrum.

The following equations are used for data manipulations if AFN (arithmetic function) is set to:

AS	absorbance subtract	SCAxAFA-CONxSCBxAFB
TS	transmission subtract	-log(SCAxAFA)-CON/(-log(SCBxAFB))
SS	spectrum subtract	-log(SCAxAFA)/(SCCxAFC)- CON(-log((SCBxAFB)/(SCCxAFC)))

APPENDIX C

When performing subtractions, the peak chosen to monitor the subractions should exist only in the spectrum from the reference sample. For example, let us assume that Figure 29 is a spectrum of silicone rubber, which will be used as the reference.

FIGURE 29. Schematic spectrum of silicone rubber

To this, protein is added. The protein spectrum alone is represented by Figure 30.

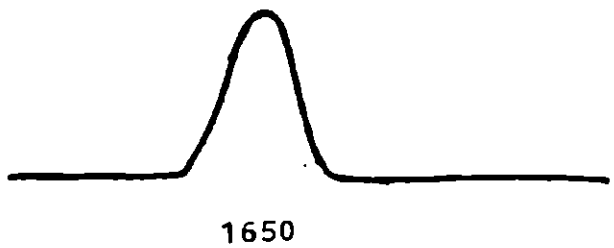

FIGURE 30. Schematic spectrum of protein

The two spectra together will appear as in Figure 31, where the 1650 cm^{-1} band comes from the protein component of the

spectrum and the 1250 cm^{-1} band is from the silicone rubber.

FIGURE 31. Schematic spectra of protein and silicone rubber

To view only the protein, the effects of the silicone rubber must be subtracted. For this, the 1250 cm^{-1} peak is monitored since it arises from the reference (silicone rubber) spectrum and not from the sample (protein) spectrum. The subtraction is continued until the 1250 cm^{-1} peak disappears as illustrated in Figure 32.

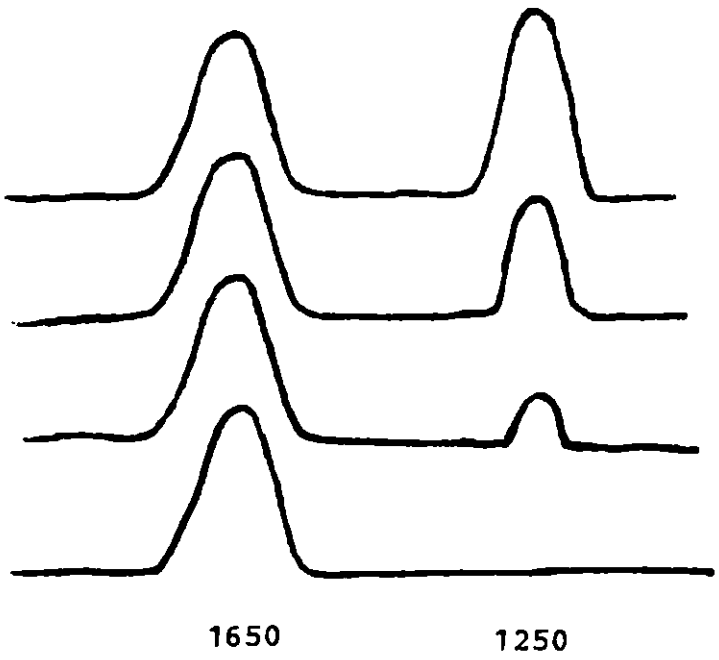

FIGURE 32. Sample subtraction

ACKNOWLEDGMENTS

I express my thanks to Dr. R. T. Greer, my major professor, for his advice and support throughout my graduate program and to Drs. Mary Helen Greer and F. Hembrough for serving on my committee. Sincere thanks is also extended to Mike Baudino, Dave Padget, Paul Antol, and Tom Boures for valuable discussions; to Steve Veysey for many hours of help aligning the ATR unit; and to Dr. Pam McAllister for surgical and photographic assistance, technical advice, and moral support. A special thanks to George Seifert for his help in preparing the figures for this thesis and his never ending encouragement.